

Model-based clock synchronization protocol

Nikolaos M. Freris, *Member, IEEE*, Vivek S. Borkar, *Fellow, IEEE*,
and P. R. Kumar *Fellow, IEEE*

Abstract

In a network of communicating nodes, each one equipped with a distinct clock, a given node is taken as reference and is associated with the time evolution t . We introduce and analyze a stochastic model for clocks in which the relative speedup of a clock with respect to the reference node, called the *skew*, is characterized by some parametrized stochastic process. We study the problem of synchronizing clocks in a network which amounts to estimating the instantaneous relative skews and relative *offsets*, i.e., the differences in the clock readouts, by asynchronously communicating time-stamped packets between neighboring nodes.

For a given communication link, we develop an algorithm for filtering the time-stamps exchanged between the two nodes in order to obtain Maximum-Likelihood (ML) estimates of the logarithm of the relative skew of one clock with respect to the other. We highlight implementation issues of the optimal filter and further present a scheme for pairwise offset estimation based on the obtained relative skew estimates. We study the properties of the proposed algorithms and provide theoretical guarantees on their performance.

We extend the analysis to the problem of network-wide synchronization where the goal is to obtain, for each node and any given time instant, estimates of its skew/offset with respect to the reference time, as well as estimates of its relative skew/offset with respect to any other clock in the network. We leverage Kalman-Bucy filtering to obtain ML estimates of the logarithm of the skews at any given time; this gives rise to an online asynchronous algorithm for optimal filtering of the time-stamps in the entire network, which is however *centralized*. To tackle this, we propose an efficient *distributed* suboptimal

N. Freris is with the School of Computer and Communication Sciences, École Polytechnique Fédérale de Lausanne, EPFL, Station 14, IC/LCAV, BC 322, Lausanne CH-1015, Switzerland, E-mail: nikolaos.freris@epfl.ch

V. Borkar is with the Department of Electrical Engineering, Indian Institute of Technology Bombay, Mumbai 400076, India, Email: borkar.vs@gmail.com

P. R. Kumar is with the Department of Electrical and Computer Engineering at Texas A&M University, Room 331E, Wisenbaker Engineering Research Center, College Station TX 77843-3259, USA. E-mail: prk@tamu.edu.

This work was submitted to IEEE/ACM Transactions on Networking–Nov. 2013.

online estimator for network-wide synchronization of skews and offsets, and study its performance both analytically and experimentally. We summarize our findings into defining a new distributed model-based clock synchronization protocol (MBCSP), and present a comparative simulation study of its accuracy versus prior art to showcase improvements.

Index Terms

Clock Synchronization, Clock Modelling, Sensor Networks, Distributed Algorithms, Stochastic Differential Equations, Random Delays, Networked Control

I. INTRODUCTION

In a large network of motes, different agents need to take actions in order for the network to perform a collaborative task as a whole. The typical paradigm is that of a *wireless sensor network* (WSN) [1] in which nodes possessing sensing, wireless communication, and computation capabilities are deployed over a large area; the sensors communicate with their neighbors wirelessly, and cooperate with each other in processing the data. Applications are ubiquitous including a) *military* e.g. monitoring forces, battlefield surveillance, targeting, damage assessment and attack reconnaissance, b) *environmental* such as habitat monitoring, fire detection, traffic control, seismography and agriculture research, c) *health* for instance monitoring patients and controlling the drug use and d) *smart homes* where sensors can help automate decisions about temperature and lighting control as well as for surveillance and safety purposes.

In such setup, centralized coordination is not an option for various reasons: first, because centralized computations typically require multi-hop communication across an identified spanning tree, which in turn implies that nodes in the proximity of a central processor will be especially burdened. More importantly, because nodes have limited energy budget such approach would lead to reduced network life-time. Last but not least, centralized computations are not robust to dynamic changes in network topology resulting from temporary link or node failures due to various reasons including mobility, fading or time-outs due to congestion. In the absence of centralized coordination, it becomes vital to achieve network-wide time synchronization among different agents.

Different clocks generally don't agree and this creates issues in determining the notion of time in a system-wide consistent fashion. The clocks in a sensor network are typically inconsistent because of frequency drifts in oscillators due to environmental conditions, such as temperature, pressure or battery voltage changes [2]. In addition, some events on specific sensors may affect the clock evolution; for example, a Berkeley mote sensor may miss clock interrupts when busy handling message transmission

or sensing tasks [3].

Many applications have stringent clock synchronization requirements. Closing control loops or coordinating events in a decentralized system [4], tracking, surveillance, target localization [5], data fusion, and scheduled operations like power-efficient duty-cycling are grounded in accurate time synchronization. Slotted communication protocols such as slotted ALOHA, TDMA scheduling or random-access MAC [6] require accurate synchronization in order to avoid unnecessary resource wastage. As we head towards the era of event-cum-time driven systems featuring the convergence of computation and communication with control, the need for well-synchronized clocks becomes increasingly important, affecting all quality-of-service (QoS), system performance or even safety, since un-coordinated actions can result in destabilizing critical networked control systems.

A commonly asked question about clock synchronization in sensornets is “why not use GPS?” Global Positioning System (GPS) has been a widespread means of synchronizing to a universal time standard. However, such centralized synchronization scheme is unapplicable in sensor network applications for various reasons. First, GPS requires a clear sky view so it does not work inside buildings, underwater, beneath dense foliage, in densely populated downtown areas with tall buildings, or even during solar flares [7]. Many sensornet motes, including the popular Berkeley mote [8], do not come equipped with a GPS receiver because of complexity and energy issues, cost and size factors [7]; the cost of a GPS receiver is multiple times that of the cheap off-the-self sensors envisioned for deploying very large WSNs of reasonable cost, while its size is also larger than the mote itself. In addition, connecting to the GPS service is too energy-consuming, multiple times than that of performing computation or wireless communication, and it can drain a sensor’s battery very fast. Finally, in adversarial environments, the GPS signals may not be trusted.

Given that centralized synchronization is not an alternative, the only option is to design and implement distributed clock synchronization algorithms for WSNs. The synchronization has stringent requirements in terms of high energy efficiency, scalability, precision (typically in the order of microseconds), robustness to node and link failures, responsiveness to clock drifts as well as low communication and computation complexity.

A. Problem setup

There is no universal definition of clock synchronization, so one needs to specify the *goal* of a synchronization algorithm. There are three main notions of clock synchronization that may be required by a particular application [2]: first, there is *ordering of events*, where the goal is to create a consistent

chronology of events in the entire network, while specification of exact time instants is not required. Then there is *relative synchronization*, aiming at estimating the time display differences among a set of clocks in the network; such information can be used to translate time-stamps from one clock to the units of any other clock. Finally there is *absolute synchronization*, seeking to set clock displays to agreement.

Another classification of synchronization algorithms is by *scope*. *Local* synchronization refers to the problem of synchronizing a node with only a subset of other nodes, typically those in its physical proximity; this is sufficient for several applications like monitoring, tracking and surveillance. For applications where the target is to achieve network-wide cooperation e.g., duty-cycling, slotted protocols or network control, it is necessary to attain *global* synchronization which involves *all* nodes in the network. In this paper, we address the most general problem of *absolute global* clock synchronization where each node calculates estimates of its skew/offset with respect to the reference clock, and can further compute estimates of its relative skew/ estimate w.r.t. any other node in the network, let alone any of its neighbors.

To achieve network clock synchronization, nodes are allowed to exchange time-stamped packets with their neighbors, i.e., with all nodes within their communication range. Such packet exchanges undergo a random communication delay that is unknown and time-varying. Here by “delay” we do not just mean the electromagnetic propagation delay, but rather the total elapsed time between the time that a sending node time-stamps a packet until the time that a receiver decodes it [2]. At the transmitter side, this typically includes the time for the operating system to process the packet after time-stamping it, followed by the time for the packet to make its way through the remainder of the communication protocol stack. Then we have electromagnetic propagation delay which is totally determinable by the distance between sender and receiver; this is in the order of a few nanoseconds for the typical case when nodes are a few meters apart. At the receiver end, there is the time it takes the packet to travel through the protocol stack plus the time taken to consult the local clock on the receipt time. Because of the randomness at the transmitter/sender side due to e.g., operating system interrupts and congestion at the MAC layer, delays are random and asymmetric in the two directions of a communication link [2]. Furthermore, the transmitter/sender delays dominate the propagation delay which is also the only deterministic component of the total delay incurred to a packet.

The ultimate goal is to develop a distributed asynchronous algorithm for the optimal filtering of time-stamps with provable performance. In the sequel, we show that *delay estimation* can be viewed a natural bi-product of clock synchronization. Estimating communication delays has many applications in its own right e.g., in predicting receipt times for network control and scheduling operations.

B. Main Results

The specific contribution that we outline in this paper is the introduction of a mathematical model for clocks and its use for developing a new clock synchronization protocol. This paper expands and extends preliminary results that appeared in [9].

In a network of $n + 1$ nodes, each equipped with its own clock, we develop a mathematical model for the time displays of different clocks and analyze its properties. We denote the display of node i 's clock at time t by $\tau_i(t)$; with no loss in generality, we assume that the time evolution t corresponds to node 0's clock, i.e., we define node 0 as the reference. We call the relative instantaneous speedup of clock i at reference time t with respect to the reference clock as its “skew,” and denote it by $a_i(t)$. The “offset” of clock i at time t is defined as the instantaneous difference of its display with respect to the reference time t , i.e., $\tau_i(t) - t$. For a given clock i , we model its skew $a_i(t)$ as a stochastic process, given by an exponential transformation of an Ornstein-Uhlenbeck process. Its time display, $\tau_i(t)$, is given by the integral of the skew $a_i(s)$ in the interval $[0, t]$. For each node, the instantaneous skew has expected value 1 at all times, while its variance is bounded by a constant; this is in alliance with experimental observations showcasing that the skew of real clocks tends to fluctuate from the nominal value in a rather controlled manner [10]. Furthermore, the time display is *unbiased*, i.e., $\mathbb{E}[\tau_i(t)] = t$ but, nonetheless, has unbounded variance which grows with time. This unbounded variance corresponds to the physical accumulation of skew errors with time [10] and makes the synchronization problem challenging. We show that if a different clock is taken as reference, the time displays of all other clocks can be expressed with respect to it using the same model, with different parameters and a change of time scales. We also calculate the Allan variance [11] of the model, which is a widely used metric for skew stability.

Under an assumption of sufficiently frequent packet exchanges and slowly-varying delays, we show how to obtain noisy relative skew measurements from one-way exchange of time-stamps in a communication link. We proceed to study the problem of pairwise synchronization, i.e., minimum-variance unbiased estimation of the logarithm of the relative skew, as an instance of linear filtering [12]. We further establish properties of and bounds on the error variance. We leverage the analysis for pairwise clock synchronization to network clock synchronization. In such a case, the differential equations that are derived for filtering are not readily implementable since they require integration with respect to the unknown reference time. To tackle this, we propose an approximation which still leads to a bounded variance filter.

We propose and analyze three schemes for the network-wide estimation of the skews. First, we consider an off-line algorithm for the filtering of pairwise estimates. We show that using the distributed scheme

of [13], [14] for the smoothing of pairwise estimates is optimal for the network-wide estimation for a particular selection of error criterion. Second, we show that the optimal linear filtering equations for the network case yield an asynchronous scheme which is stable and of bounded variance, but in general requires centralized computations. Last and more importantly, we derive a suboptimal asynchronous scheme which is readily implementable in a decentralized fashion.

We address protocol implications and present a scheme to estimate relative offset estimates based on estimates of the relative skews. We summarize our findings into defining *model-based clock synchronization protocol* (MBCSP), and further present a comparative simulation study with both synthetic and real data in order to showcase improvement over previous art.

II. RELATED LITERATURE

The simplest yet most commonly adopted model for clocks is the so called *affine* model. In this model, the skew is assumed *constant*, at least for the duration of a synchronization period; in practice, this implies that synchronization has to be carried out at faster time-scale than the rate of clock drifts. The display of the i -th clock satisfies $\tau_i(t) := a_i(t - t_0) + b_i$, where t denotes the reference time evolution, $a_i > 0$ is the skew of clock i , and $b_i \in \mathbb{R}$ is the offset of the clock at reference time t_0 . A complete analysis of the feasibility of the problem for the case of *affine* clocks was carried out in [2]. It was shown that clock synchronization is *impossible* even for the best case scenario of a complete graph and constant (but unknown) link delays, and the uncertainty set was fully characterized. The majority of existing synchronization protocols considers constant skew for fixed time periods, and accounts for skew drifts by adaptively estimating a_i for each given time interval.

For a comprehensive survey on clock synchronization with emphasis on sensor network applications we refer the reader to [7], [15], [16]. In the sequel, we overview related work featuring popular synchronization protocols, as well as theoretical results on the topic.

In large networks where synchronization requirements are not too stringent, e.g. the Internet, the Network Time Protocol (NTP [17]) has been successfully used for over two decades. NTP is a *hierarchical* protocol used to synchronize with external sources (typically via GPS) organized in a hierarchy of levels, called *strata*. It attains accuracy in the order of a few milliseconds [17]. However, real-time applications in wireless sensor networks typically require precision in the order of a few microseconds, so NTP is no longer applicable in this setup.

For accurate synchronization in sensor networks a variety of algorithms have been suggested. Reference Broadcast Synchronization (RBS [18]) is a *receiver-receiver* synchronization algorithm which exploits

the broadcast nature of the wireless medium. In RBS, nodes broadcast packets without any time-stamping on the transmitter side. The nodes that receive the same transmitted packet record the reception times and exchange this information with their neighbors so as to estimate their clock difference; an implicit assumption is that the one-way delays are the same for neighboring nodes, which completely eliminates the transmitter-side non-determinism and accuracy depends mainly on the difference of receiver processing delays. This scheme was tested in sensor networks comprising of Berkeley motes using off-the-shelf 802.11 Ethernet, and achieved precision within $11 \mu s$ [18]. The Timing-Sync Protocol for Sensor Networks (TPSN [8]) is a popular *sender-receiver* synchronization protocol which uses time-stamping at the MAC layer to eliminate the transmission delay which is typically the most variable term in wireless sensor networks. It was observed and verified by simulations [8] that TPSN achieves approximately twice the accuracy of RBS for pairwise synchronization. TPSN uses message-passing across a spanning tree to achieve network-wide synchronization. In [19], authors identify the sources that contribute to packet delivery delay and propose the Flooding Time Synchronization Protocol (FTSP [19]). FTSP uses hardware solutions and an efficient time-stamping mechanism to effectively eliminate all packet delay factors but the propagation delay. Linear regression is used to compensate for clock drifts, and the achieved precision was measured $10 \mu s$ on average, for a network with several hundreds of nodes. Moreover, FTSP was found to be highly robust to link failures, and dynamic readjustments of the reference node [19].

A widely studied problem is that of obtaining *consistent* estimates for clock's offsets, given estimates of relative measurements between any two communicating nodes [13], [14], [20]–[26]; a comprehensive survey can be found in [27]. The term “consistent” means that estimates should satisfy Kirchoff's voltage law, i.e., should sum to zero along the edges of a directed cycle. This constraint leads to *smoothing* pairwise measurements and is also used for obtaining nodal skew estimates by considering relative measurements of the logarithm of clock's skew. Karp et al. [20] derived the *best linear unbiased estimate* (BLUE) of the pairwise offset differences between any two nodes (i, j) , where “best” refers to minimum-variance. They further established that the variance of the BLUE is equal to the effective *resistance* between those two nodes in an electric network where the resistance of each link is equal to the error variance of the corresponding relative measurement. The connection of BLUEs with resistance networks has also been thoroughly studied in [13], [22], [24]; the authors therein studied the asymptotic variance for large networks and established sharp scaling laws for various classes of graphs. It follows from the electrical analogy that there is a great merit in leveraging all relative measurements not just those along a spanning tree as in TPSN [8]. For example, for connected random planar networks the asymptotic variance of the BLUE between any two nodes is $O(1)$ [22], while for a tree it is $O(\sqrt{n})$; this provides

theoretical support for the feasibility of clock synchronization in large networks.

A large emphasis has been given on developing distributed asynchronous schemes for iteratively calculating the BLUEs by *smoothing* relative measurements. One such scheme was developed in [20] under the restrictive assumption of Gaussian measurement noise. An asynchronous version of the Jacobi algorithm, which essentially amounts to computing the pseudo-inverse of the weighted reduced Laplacian of the network graph in a decentralized fashion, was developed simultaneously and independently in [14], [21]; The achieved average accuracy was measured to be $2\mu s$ for pairwise synchronization, and $20\mu s$ for a network of 40 nodes, in which FTSP achieved an average accuracy of $30\mu s$ [21]. In [23], it was proposed to use information from the two-hop neighborhood of each node for deriving a distributed algorithm called *Overlapping Subgraph Estimator*; the convergence to BLUE was established and it was argued that this scheme has a faster convergence speed, therefore leading to energy savings in a sensor network. Barooah et al. [23] also proposed an efficient method for initializing the nodal estimates, called *flagged initialization*, which led to reducing the number of iterations (for a given convergence criterion) in all tested scenarios. Giridhar and Kumar [13], [22] obtained bounds on the convergence rate of the *spatial smoothing* algorithm, i.e., the Jacobi algorithm applied to least-squares estimation. They made connections of the convergence rate with two graph indices, namely the degree of the root node and the *edge-connectivity*, by using Cheeger's inequality. For example, for either lattices or random planar graphs, it was shown that the number of iterations required to attain a given accuracy is $O(n^2)$ [22]. An implicit assumption of the aforementioned approaches is that communications links are symmetric. When this assumption is violated, it was shown in [25] that the distributed Jacobi algorithm converges to a suboptimal unbiased estimate. The case where network topology is varying, e.g. due to mobility, was studied in [26] where convergence was established using results from Markov Jump Linear Systems. Distributed synchronization algorithms are directly related to consensus; algorithms based on average consensus have been proposed in [3], [28], while [29] proposed a protocol based on maximum-value consensus. Last but not least, a class of randomized distributed smoothing algorithms with provable exponential convergence in the mean square appeared in [30].

Further related literature treats the case of *atomic* clocks. A model for atomic clocks was proposed in [31], [32]; The authors suggested linear stochastic differential equation systems where the state variables correspond to the phase and frequency deviations of the clock oscillator. As a metric for clock stability, an index of the quadratic variation of the clock frequency called *Allan variance* was introduced in [11] and was calculated for the particular clock model in [32].

III. STOCHASTIC CLOCK MODEL

In a network of $n + 1$ clocks, we consider a reference time, denoted by the non-negative continuous variable $t \in \mathbb{R}_+$. Without any loss in generality, we assume that the reference corresponds to a given clock, say clock 0. We use $\tau_i(t)$ to denote the display of the i -th clock at time t . To model such time displays $\tau_i(t)$, we define independent Ornstein-Uhlenbeck processes [33] $\{X_i(\cdot)\}_{i=1}^n$:

$$dX_i(t) = -\alpha_i X_i(t)dt + \epsilon_i dW_i(t) \quad ; \quad X_i(0) = 0, \quad (1)$$

where $\{W_i(\cdot)\}_{i=1}^n$ are independent scalar Brownian motions and where $\alpha_i, \epsilon_i > 0$ are given constants. Let $a_i(t)$ denote the *skew* of the i -th node at time t , i.e., its relative speed with respect to the reference clock. We model the skew as

$$a_i(t) := c_i(t)e^{X_i(t)}, \quad c_i(t) := e^{-\frac{1}{4} \frac{\epsilon_i^2}{\alpha_i} (1 - e^{-2\alpha_i t})} \quad (2)$$

Then the clock display $\tau_i(t)$ is given by

$$\tau_i(t) := \int_0^t a_i(t')dt'; \quad \tau_i(0) = 0. \quad (3)$$

Remark 1. The model also applies for the reference clock 0, by setting $\epsilon_0 = 0$. We have assumed that all clocks start *synchronized* in the sense that $\tau_i(0) = 0, a_i(0) = 1$, and that synchronization is lost as an effect of time-varying skews; the extension to the general case is straightforward. Note that $a_i(t) > 0 \forall t \geq 0, i = 0, 1, \dots, n$, which implies that for all clocks the time displays $\tau_i(t)$ are strictly increasing functions of t , i.e., the time at each clock evolves *forward*.

Remark 2 (Stochastic differential equation for the skew). It follows as an application of Itô's formula [12] and the definition (2) that the skew $a_i(t)$ satisfies the following Stochastic Differential Equation (SDE):

$$da_i(t) = (-\alpha_i \log a_i(t) + \frac{1}{4} \epsilon_i^2 (3 - e^{-2\alpha_i t}))a_i(t)dt + \epsilon_i a_i(t)dW_i(t). \quad (4)$$

Remark 3 (Numerical simulation of OU process). The Ornstein-Uhlenbeck process $X_i(t)$ can be numerically approximated by a discrete process $\bar{X}_i(k)$ defined recursively by

$$\bar{X}_i((k + 1)) = (1 - \alpha_i \Delta t)\bar{X}_i(k) + \epsilon_i \sqrt{\Delta t} w_i(k), \quad (5)$$

where Δt is the stepsize, $\bar{X}_i(k)$ denotes the numerical approximation of $X_i(k\Delta t)$ and $\{w_i(k)\}$ represents a sequence of independent standard normal random variables. For the linear SDE under consideration (OU), this method corresponds to both Euler-Maruyama and Milstein's methods [34]. In particular the

numerical approximation (5) has *strong order of convergence* $\gamma = 1$, in the sense that for a fixed interval $[0, T]$ there exists $C(T) > 0$ such that

$$\mathbb{E}|\bar{X}_i(n) - X_i(n\Delta t)| \leq C(T)\Delta t^\gamma, \quad (6)$$

for all $n = 0, 1, \dots, \lfloor \frac{T}{\Delta t} \rfloor$.

However, for the OU case, an exact calculation is possible at discrete values as follows. From the analysis in appendix A it follows that for any $t \geq 0$ we have

$$X_i(t) = \epsilon_i \int_0^t e^{-\alpha_i(t-s)} dW_i(s), \quad (7)$$

whence for $t_2 \geq t_1 > 0$

$$X_i(t_2) = e^{-\alpha_i(t_2-t_1)} X_i(t_1) + \int_{t_1}^{t_2} e^{-\alpha_i(t_2-s)} dW_i(s), \quad (8)$$

in particular we can consider again a uniform sampling with step Δt and get

$$\bar{X}_i(k+1) = e^{-\alpha_i \Delta t} \bar{X}_i(k) + \sqrt{\frac{1}{2\alpha_i} [1 - e^{-2\alpha_i \Delta t}]} v_i(k), \quad (9)$$

where $v_i(k)$ is standard (mean zero and unit variance) Gaussian White Noise (GWN) sequence.

A. Model Properties

In this section, we summarize the main properties of the proposed mathematical model. In particular, we show that, for each clock, the instantaneous skew has mean value 1 at all times, and bounded variance. However, the variance of the time display grows unbounded. We further show how to express the time of one clock with respect to the time of another, which comes handy in the case that the reference may be dynamically re-selected to account for changes in network topology such as broken links/nodes.

Lemma 1 (Properties of the stochastic model). *For each clock $i = 1, 2, \dots, n$:*

- 1) *The skew satisfies $\mathbb{E}[a_i(t)] = 1, \forall t \in \mathbb{R}_+$, and $\sup_{t \in \mathbb{R}_+} \text{Var}(a_i(t)) < +\infty$.*
- 2) *The time display satisfies $\mathbb{E}[\tau_i(t)] = t, \lim_{t \rightarrow +\infty} \text{Var}(\tau_i(t)) = +\infty$; in particular, $\text{Var}(\tau_i(t)) = \Omega(t), \text{Var}(\tau_i(t)) = O(t^2)$.*

Proof: The proof can be found in Appendix A. ■

Remark 4 (Metric for clock's quality). One may use either $\frac{\alpha_i}{\epsilon_i^2}$ or $\frac{\alpha_i}{\epsilon_i}$ as a metric for the “quality” of the i -th clock. This is justified by noting that the asymptotic skew variance as well as the upper bound on the variance of the time display of clock i , is increasing in $e^{\frac{\epsilon_i^2}{\alpha_i}}$, while the lower bound on $\text{Var}(\tau_i(t))$ is

increasing in $\frac{\alpha_i}{\epsilon_i}$, cf. (A-97), (A-105) in appendix A. In conclusion, the expected deviation of the clock from nominal values is decreasing in each metric.

The following result characterizes the sample path behavior of the skew process $a_i(t)$.

Theorem 2 (Sample path properties of skew). *The skew $a_i(t)$ almost surely satisfies*

$$\overline{\lim}_{t \rightarrow +\infty} a_i(t) = \sup_{t \geq 0} a_i(t) = +\infty \quad (10)$$

$$\underline{\lim}_{t \rightarrow +\infty} a_i(t) = \inf_{t \geq 0} a_i(t) = 0. \quad (11)$$

Proof: It follows from (A-94) that $Y_i(t) := e^{\alpha_i t} X_i(t) = \epsilon_i \int_0^t e^{\alpha_i s} dW_i(s)$ is a continuous local martingale [33], with quadratic variation $[Y_i, Y_i]_t = e^{2\alpha_i t} - 1$, and $Y_i(0) = 0$. Hence the Dambis, Dubin-Schwartz theorem [33], applies and yields that $Y_i(t) = \tilde{W}_i([Y_i, Y_i]_t)$, where $\{\tilde{W}_i(t)\}$ is a standard Brownian motion; in particular, $X_i(t) = \epsilon_i e^{-\alpha_i t} \tilde{W}_i(e^{2\alpha_i t} - 1)$. It follows from the law of iterated logarithms [35] which states that for Brownian motion $\{W(t)\}$ it holds that $\overline{\lim}_{t \rightarrow +\infty} \frac{|W(t)|}{\sqrt{2t \log \log t}} = 1, a.s.$ that $\overline{\lim}_{t \rightarrow +\infty} X_i(t) = +\infty, \underline{\lim}_{t \rightarrow +\infty} X_i(t) = -\infty, a.s.$ ■

A particular realization of the clock display according to our model, as well as a plot of its variance are illustrated in Section X.

B. Time translation among different clocks

We show how to translate time among different (non-reference) clocks i and j , i.e., how to express the time of one non-reference clock in the units of another clock.

Proposition 3 (Time translation). *Assume that $\alpha_i = \alpha_j = \alpha$, and consider the time of the j -th clock expressed with respect to the time of the i -th clock; formally let $\tilde{\tau}_{ji} := \tau_j \circ \tau_i^{-1}$, i.e., $\tilde{\tau}_{ji}(\tau) := \tau_j(\tau_i^{-1}(\tau))$.*

Then

1) $\tilde{\tau}_{ji}(\tau)$ satisfies the differential equation

$$d\tilde{\tau}_{ji}(\tau) = \frac{a_j(t)}{a_i(t)} d\tau, \quad (12)$$

where $t = \tau_i^{-1}(\tau)$.

2) For $i, j \neq 0$, let $X_{ij}(t) := X_j(t) - X_i(t)$. Then $X_{ij}(t)$ satisfies the SDE

$$dX_{ij}(t) = -\alpha X_{ij}(t) dt + \epsilon_{ij} dW_{ij}(t) ; X_{ij}(0) = 0, \quad (13)$$

and the “relative skew” is given by

$$a_{ij}(t) := \frac{a_j(t)}{a_i(t)} = c_{ij}(t) e^{X_{ij}(t)}, \quad (14)$$

where $c_{ij}(t) := \frac{c_j(t)}{c_i(t)} = c_{ij} e^{\frac{1}{4}(\frac{\epsilon_j^2}{\alpha} - \frac{\epsilon_i^2}{\alpha})e^{-2\alpha t}}$, $c_{ij} := e^{-\frac{1}{4}(\frac{\epsilon_j^2}{\alpha} - \frac{\epsilon_i^2}{\alpha})}$, $\epsilon_{ij} := (\epsilon_i^2 + \epsilon_j^2)^{\frac{1}{2}}$, and $W_{ij}(t)$ is a standard scalar Brownian motion dependent on $W_i(t), W_j(t)$.

3) Let $\tilde{X}_{ij}(\tau) := X_{ij}(\tau_i^{-1}(\tau))$. Then $\tilde{X}_{ij}(0) = 0$ and

$$d\tilde{X}_{ij}(\tau) = -\alpha \frac{1}{a_i(t)} \tilde{X}_{ij}(\tau) d\tau + \epsilon_{ij} \frac{1}{\sqrt{a_i(t)}} dW_{ij}(\tau), \quad (15)$$

where $t := \tau_i^{-1}(\tau)$.

Proof: The function $\tau_i(t)$ is strictly increasing and continuous on \mathbb{R}_+ , and tends to infinity. Therefore, it is bijective so the inverse $\tau_i^{-1}(\tau)$ exists and is also strictly increasing. By the chain rule, we have that $\frac{d}{d\tau} \tau_j(\tau_i^{-1}(\tau)) = \dot{\tau}_j(t) \frac{d}{d\tau} \tau_i^{-1}(\tau) = a_j(t) \frac{1}{\dot{\tau}_i(t)} = \frac{a_j(t)}{a_i(t)}$, where $t := \tau_i^{-1}(\tau)$ and we used the notation $\dot{f}(t) := \frac{d}{dt} f(t)$. To prove the second part, note that the SDE (1) is simply a shorthand for the stochastic integral equation

$$X_i(t) = -\alpha_i \int_0^t X_i(t') dt' + \epsilon_i W_i(t). \quad (16)$$

Then, since $\alpha_i = \alpha_j = \alpha$, it follows that $\frac{a_j(t)}{a_i(t)} = c_{ij}(t) e^{X_{ij}(t)}$ and the result follows from

$$X_{ij}(t) = -\alpha \int_0^t X_{ij}(t') dt' + \epsilon_j W_j(t) - \epsilon_i W_i(t), \quad (17)$$

and Levy's characterization of Brownian motion [33]. The last part follows by a time-scale change in the equation

$$X_{ij}(t) = -\alpha \int_0^t X_{ij}(t) dt + \epsilon_{ij} W_{ij}(t). \quad (18)$$

Setting $\tilde{X}_{ij}(\tau) := X_{ij}(\tau_i^{-1}(\tau))$ we get

$$\tilde{X}_{ij}(\tau) = -\alpha \int_0^{\tau_i^{-1}(\tau)} X_{ij}(\tau') d\tau' + \epsilon_{ij} W_{ij}(\tau_i^{-1}(\tau)). \quad (19)$$

Using the change of variable $t' = \tau_i^{-1}(\tau')$ we get that the drift term $-\alpha \int_0^{\tau_i^{-1}(\tau)} X_{ij}(\tau') d\tau'$ becomes $-\alpha \int_0^t \frac{1}{a_i(t')} \tilde{X}_{ij}(t') dt'$. Since $a_i(t)$ is characterized by a bijective transformation of $X_i(t)$ it is progressively measurable with respect to the filtration $\sigma(W_{ij}(t)) := \sigma(W_i(t)) \vee \sigma(W_j(t))$ [35]. Hence it follows that $M_\tau := \int_0^\tau \frac{1}{\sqrt{a_i(t')}} dW_{ij}(\tau')$, for $t' = \tau_i^{-1}(\tau')$, is a continuous local martingale [33], $M(0) = 0$, and its quadratic variation is $[M, M]_\tau = \tau_i^{-1}(\tau)$. By the celebrated Dambis, Dubin-Schwartz theorem [33] $M_\tau = W_{ij}([M, M]_\tau) = W_{ij}(\tau_i^{-1}(\tau))$. ■

¹Note that in the case that $j = 0$ we should set $\epsilon_{i0} = -\epsilon_i$, but this would not alter the distribution of the solution of the SDE.

Remark 5 (Relative skew properties). From (13), (14), (A-95) it follows that it is not true that $\mathbb{E}[a_{ij}(t)] = 1$ nor that $\mathbb{E}[a_{ij}(t)]\mathbb{E}[a_{ji}(t)] = 1$:

$$\mathbb{E}[a_{ij}(t)] = c_{ij}(t)e^{\frac{1}{2}\mathbb{E}[X_{ij}^2(t)]} = e^{\frac{\epsilon_i^2}{2\alpha}(1-e^{-2\alpha t})} > 1, \quad (20)$$

$$\mathbb{E}[a_{ij}(t)]\mathbb{E}[a_{ji}(t)] \nearrow e^{\frac{\epsilon_i^2 + \epsilon_j^2}{2\alpha}} > 1. \quad (21)$$

Remark 6 (Convention). Since the “quality” of a clock i is characterized by the quantity $\frac{\alpha_i}{\epsilon_i^2}$ or $\frac{\alpha_i}{\epsilon_i}$, while in order to define the translation equations for the nodes i, j we needed $\alpha_i = \alpha_j$, we henceforth adopt for simplicity the convention that $\alpha_i \equiv \alpha$ for all $i = 1, \dots, n$. The “quality” is then modeled solely by ϵ_i , so we still allow for diverse clocks. Recall that α models the transient behavior, cf. (A-95).

Corollary 4 (L^p –boundedness). *For any $p \geq 1$, the processes $X_i(t), X_{ij}(t)$ are L^p – bounded Gaussian processes; the processes $a_i(t), a_{ij}(t), \frac{1}{a_i(t)}, \frac{1}{a_{ij}(t)}$ are also $L^p(P)$ – bounded.*

Proof: The case where $i = j = 0$ is trivial, since then $X_0(t) \equiv 0, a_0(t) \equiv 1$. The Ornstein-Uhlenbeck SDE is a linear SDE, hence the processes $X_i(t), X_{ij}(t)$ are Gaussian, mean 0, and by (A-95), they have uniformly bounded variance. The rest follows from (2), (14). ■

C. Allan variance

Allan variance is as a performance index for clock stability. Consider the average skew of the i -th clock in the interval $[t - T, t]$:

$$\bar{a}_i(t) := \frac{1}{T} \int_{t-T}^t a_i(t') dt' = \frac{\tau_i(t) - \tau_i(t-T)}{T}. \quad (22)$$

The Allan variance $\sigma_{a_i}^2(T)$ is defined by [11]

$$\sigma_{a_i}^2(T) := \frac{1}{2} \lim_{T' \rightarrow \infty} \frac{1}{T'} \int_0^{T'} (\bar{a}_i(t+T) - \bar{a}_i(t))^2 dT', \quad (23)$$

provided that the limit exists.

Remark 7 (Numerical approximation of Allan variance). In practice, the Allan variance is approximated based on $N + 1$ periodic measurements of clock i 's display with period T by:

$$\sigma_{a_i}^2(T) \simeq \frac{1}{2N} \sum_{k=1}^N (\bar{a}_i((k+1)T) - \bar{a}_i(kT))^2, \quad (24)$$

where N is sufficiently large. In the case of the proposed stochastic model the Allan variance can be defined as

$$\sigma_{a_i}^2(T) := \frac{1}{2} \lim_{t \rightarrow \infty} \mathbb{E}[(\bar{a}_i(t+T) - \bar{a}_i(t))^2], \quad (25)$$

where we have used the ergodicity of the OU process [33]. Using (25), (22) and (A-102) we get

$$\sigma_{a_i}^2(T) = \frac{1}{T^2} \left(\int_0^T \int_0^T e^{\frac{\epsilon_i^2}{2\alpha_i}} e^{-\alpha_i|t-s|} ds dt - \int_0^T \int_{-T}^0 e^{\frac{\epsilon_i^2}{2\alpha_i}} e^{-\alpha_i|t-s|} ds dt \right). \quad (26)$$

Remark 8. Note that the Allan variance is not equal to the sample variance of the skew process. It is also different than $\lim_{t \rightarrow \infty} \frac{1}{2} \mathbb{E}[(a_i(t+T) - a_i(t))^2]$, which for our model is equal to $e^{\frac{\epsilon_i^2}{2\alpha_i}} - e^{\frac{\epsilon_i^2}{2\alpha_i}} e^{-\alpha_i T}$, an increasing function of T . We will refer to this quantity as ‘‘asymptotic skew difference variance’’.

Remark 9 (System identification). Based on a numerical approximation of Allan variance through periodic measurements (as in Remark 7) parameters α_i, ϵ_i can be estimated using standard curve-fitting optimization techniques and the analytical formula (26).

IV. MEASUREMENT MODEL

We model the communication network with a graph $G = (V, E)$. Node i can send packets to node j if and only if $(i, j) \in E$. We allow such pair of nodes to exchange time-stamped packets. When a node i sends its k -th packet, it includes a time-stamp of the sent time according to its own clock, $s_i^{(k)}$. We allow for broadcast, i.e., for a sending packet to be received by two neighboring nodes. When node j receives this time-stamped packet it records the time according to its clock of when it received the packet, $r_{i,j}^{(k)}$. We assume that a packet sent over a link (i, j) undergoes a delay of $d_{ij}^{(k)}$ time units (as measured by the reference clock); recall that this includes not only the electromagnetic propagation delay, but rather the total elapsed time between time-stamping at the transmitter side and time-stamping at the receiver end [2]. Delays are typically random and asymmetric [2]; in general, $d_{ij} \neq d_{ji}$ and $d_{ij} \neq d_{il}$ for $(i, j), (j, i), (i, l) \in E$. Note also that the time instants when a time-stamped message is sent are typically determined based on the sender clocks, and are therefore stochastic.

To obtain a noisy measurement of the relative skew a_{ij} , node i needs to send two consecutive time-stamped packets to node j ; this communication scheme is depicted in Figure 1. The measurement model we adopt is summarized in the next theorem; the analysis can be found in appendix B.

Theorem 5 (Measurement at a link (i, j)).

In a link (i, j) , node j can make a noisy measurement of the logarithm of the relative skew at time t_k , $a_{ij}(t_k)$, by sending two consecutive packets at times t_k, t_{k+1} and using all four send and receive time-stamps. The measurement is of the form

$$y_{ij}(t_k) := X_{ij}(t_k) + v_{ij}(t_k), \quad (27)$$

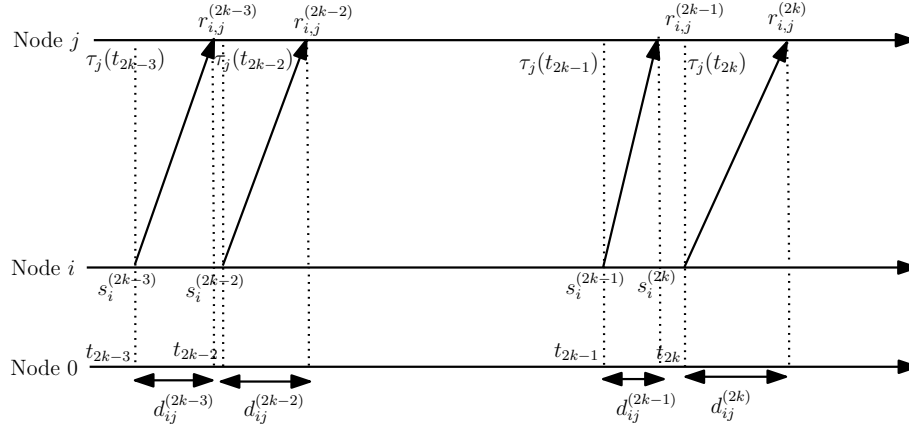


Fig. 1. Communication via exchange of time-stamped packets

where ²

$$y_{ij}(t_k) := \log \left| \frac{r_{i,j}^{(k+1)} - r_{i,j}^{(k)}}{s_i^{(k+1)} - s_i^{(k)}} \right| - \frac{1}{4} \left(\frac{\epsilon_j^2}{\alpha} - \frac{\epsilon_i^2}{\alpha} \right) (1 - e^{-2\alpha t_k}), \quad (28)$$

and $v_{ij}(t_k) \sim \mathcal{N}(0, \sigma_{ij}^2(t_k))$, is white Gaussian noise.

V. PAIRWISE SYNCHRONIZATION OF TWO CLOCKS

We show how to filter the time-stamps in a directed link (i, j) in order to derive the ML estimate of the relative skew $a_{ij}(t)$. In this section, we use t_k to denote the time instant (measured in the units of the reference time) at which the k -th measurement is made; this corresponds to t_{2k} for the scheme shown in Figure 1. This problem reduces to the continuous-discrete linear filtering problem [12], for the system

$$dX_{ij}(t) = -\alpha X_{ij}(t)dt + \epsilon_{ij}dW_{ij}(t); \quad X_{ij}(0) = 0, \quad (29)$$

$$y_{ij}(t_k) = X_{ij}(t_k) + v_{ij}(t_k); \quad v_{ij}(t_k) \sim \mathcal{N}(0, \sigma_{ij}^2(t_k)), \quad (30)$$

The ML estimate can be computed by the discrete Kalman-Bucy filter³

$$d\hat{X}_{ij}(t) = -\alpha \hat{X}_{ij}dt, \quad t \geq 0; \quad \hat{X}_{ij}(0) = 0, \quad (31)$$

$$\hat{X}_{ij}(t_k^+) = \hat{X}_{ij}(t_k^-) + K(t_k)(y_{ij}(t_k) - \hat{X}_{ij}(t_k^-)), \quad (32)$$

$$K(t_k) = \frac{P_{ij}^{t_k^-}(t_k)}{P_{ij}^{t_k^-}(t_k) + \sigma_{ij}^2(t_k)}. \quad (33)$$

²For a link (i, j) such that $i, j \neq 0$, we could also ignore $e^{-2\alpha t_k}$, because neither i nor j has access to t . The error of such approximation is negligible for large values of t , and is dominated by the noise term.

³Throughout, we use the standard notation for estimates and conditional-unconditional error variances as in [12].

The conditional error variance is equal to the unconditional error variance $P_{ij}(t) := \mathbb{E}[(X_{ij}(t) - \hat{X}_{ij}(t))^2] = \mathbb{E}[P_{ij}^t(t)]$ [12]. It satisfies

$$\frac{dP_{ij}^t(t)}{dt} = -2\alpha P_{ij}^t(t) + \epsilon_{ij}^2, \quad t \geq 0, \quad (34)$$

$$P_{ij}^{t_k^+}(t_k) = \frac{\sigma_{ij}^2(t_k)}{P_{ij}^{t_k^-}(t_k) + \sigma_{ij}^2(t_k)} P_{ij}^{t_k^-}(t_k). \quad (35)$$

The optimal filter is uniformly asymptotically stable, cf. (31), and has uniformly bounded variance, since the unconditional state variance is uniformly bounded, cf. Lemma 1.1.

Remark 10 (Estimation of relative skew). The estimate $\hat{X}_{ij}(t)$ and its error variance $P_{ij}^t(t)$ can be used to obtain the optimal estimate for the relative skew $a_{ij}(t)$. This is because the conditional distribution of $X_{ij}(t)$ given the measurements at time t , $\mathcal{Y}_t := \{y_{ij}(t_k)\}_{t_k \leq t} \cup \{y_{ji}(t_k)\}_{t_k \leq t}$, is $\mathcal{N}(\hat{X}_{ij}(t), P_{ij}^t(t))$. Hence

$$\mathbb{E}[a_{ij}(t)|\mathcal{Y}_t] = c_{ij}(t)\mathbb{E}[e^{X_{ij}(t)}|\mathcal{Y}_t] = c_{ij}(t)e^{\hat{X}_{ij}(t) + \frac{1}{2}P_{ij}^t(t)}. \quad (36)$$

This estimate has uniformly bounded conditional and unconditional variance, as well.

Remark 11 (Antisymmetry property). From the filtering equations one can easily check that if we define the measurement $y_{ji}(t_k) := -y_{ij}(t_k)$, and assume that $\sigma_{ij}^2(t_k) = \sigma_{ji}^2(t_k)$, then for all $t \geq 0$ we have that $\hat{X}_{ji}(t) = -\hat{X}_{ij}(t)$, $P_{ij}(t) = P_{ji}(t)$. This means that the optimal estimates can be, in principle, obtained by both communicating nodes. We further study the implementation of the filter in the next section.

Theorem 6 (Filter error variance). *The error variance of the optimal filter satisfies*

$$\bar{P} \leq \frac{1}{2}[-(1-A)(\Sigma^2 - E) + \sqrt{(1-A)^2(\Sigma^2 - E)^2 + 4(1-A)E\Sigma^2}], \quad (37)$$

where $E := \frac{\epsilon_{ij}^2}{2\alpha}$, $A = e^{-2\alpha\bar{T}}$ and $\bar{P}, \bar{T}, \Sigma^2$ denote either the supremum or limit superior of $P_{ij}(t), t_{k+1} - t_k, \sigma_{ij}^2(t_k)$, respectively. In particular,

$$\lim_{\sup(t_{k+1}-t_k) \rightarrow 0} \sup_{t \geq 0} P_{ij}(t) = 0. \quad (38)$$

Proof: It follows from (34) that for $t \in [t_k, t_{k+1})$

$$P_{ij}^t(t) = (P_{ij}^{t_k^+}(t_k) - E)e^{-2\alpha(t-t_k)} + E \leq (P_{ij}^{t_k^+}(t_k) - E)A + E, \quad (39)$$

since $P_{ij}(t) \leq E$ for all $t \geq 0$. From (35), we get that

$$P_{ij}^{t_k^+}(t_k) = \frac{1}{\frac{1}{P_{ij}^{t_k^-}(t_k)} + \frac{1}{\sigma_{ij}^2(t_k)}}. \quad (40)$$

Substituting this into (39) and taking sup or $\overline{\lim}$ in both sides of the resulting equation yields the inequality $\bar{P} \leq (\frac{1}{\bar{P} + \bar{\Sigma}^2} - E)A + E$. Solving this equation leads to a quadratic equation. The upper bound is obtained the largest solution of the quadratic equation (which is positive and the quadratic is increasing at that point). \blacksquare

A. Implementation issues

In an actual implementation the optimal estimator is run by receiving node j . We point out an issue in that node j does not know the reference time evolution t , which is in fact the unknown it effectively seeks to estimate. Therefore it cannot run the differential equations (31), (34).

To tackle this, we propose a practical fix which leads to a stable filter with uniformly bounded error variance. Define $\tilde{X}_{ij}(\tau) := \hat{X}_{ij}(\tau_j^{-1}(\tau))$, where again $t = \tau_j^{-1}(\tau)$. It follows directly from (1) that

$$\frac{d\tilde{X}_{ij}(\tau)}{d\tau} = -\alpha \frac{1}{a_j(t)} \tilde{X}_{ij}(\tau). \quad (41)$$

Note that $a_j(t)$ is a random process, which is not measurable by j , therefore (41) is not an ordinary differential equation. Let us define the suboptimal filter

$$\frac{d\bar{X}_{ij}(\tau_j)}{d\tau} = -\alpha \frac{1}{f_j(\tau)} \bar{X}_{ij}(\tau), \quad (42)$$

where $f_j(t)$ is measurable with respect to $\mathcal{Y}_{ij}^t := \{y_{ij}(t_k)\}_{t_k \leq t} \cup \{y_{ji}(t_k)\}_{t_k \leq t}$ and $f_j(t) > 0$ holds a.s. For simplicity, we may set $f_j(t) = 1 = \mathbb{E}[a_j(t)]$ or $f_j(t) = \mathbb{E}[a_j(t)|\mathcal{Y}_{ij}^t]$ but the analysis holds for any a.s. positive \mathcal{Y}_{ij}^t -measurable function. For any such $f_j(t)$ we obtain a filter with bounded unconditional error covariance provided that, as before, the noise variance is uniformly bounded.

Theorem 7 (Properties of the suboptimal filter). *Let the suboptimal estimator $\bar{X}_{ij}(\tau_j)$ run at node j*

$$\frac{d\bar{X}_{ij}(t)}{dt} = -\frac{a_j(t)}{f_j(t)} \alpha \bar{X}_{ij}(t), \quad (43)$$

where $f_j(t)$, is a \mathcal{Y}_{ij}^t -measurable random variable such that $f_j(t) > 0$, a.s. At a measurement let

$$\bar{X}_{ij}(t_k^+) = \bar{X}_{ij}(t_k^-) + k(t_k)(y_{ij}(t_k) - \bar{X}_{ij}(t_k^-)), \quad (44)$$

where $k(t_k) \in [0, 1]$ is a $\mathcal{Y}_{ij}^{t_k}$ -measurable random variable, and $y_{ij}(t_k)$ is the measurement as in Theorem 5. Assume that the measurement error variance sequence satisfies

$$\sup_k \sigma_{ij}^2(t_k) = \Sigma^2 < +\infty, \quad (45)$$

Then, the filter is uniformly asymptotically stable and has bounded unconditional error variance for any selection of $f_j(t) > 0$ and $\{k(t_k)\} \subset [0, 1]$.

Proof: The fact that $\bar{X}_{ij}(t)$ is uniformly asymptotically stable follows directly by using the Lyapunov function $V(x) = \frac{1}{2}x^2$, in (43). To establish boundedness of the unconditional error variance, note the useful inequality $\bar{P}_{ij}(t) \leq 2\mathbb{E}[\bar{X}_{ij}^2(t)] + 2\mathbb{E}[X_{ij}^2(t)]$; in addition, $X_{ij}(t)$ is L^2 -bounded and $\mathbb{E}[X_{ij}^2(t)] \leq \frac{\epsilon_i^2 + \epsilon_j^2}{2\alpha}$ (cf. Prop. 3, and (A-95)).

In an interval between two measurements, $t \in [t_{k-1}, t_k)$, it holds:

$$\bar{X}_{ij}^2(t) = \bar{X}_{ij}^2(t_{k-1})e^{-2\alpha \int_{t_{k-1}}^t \frac{a_j(t)}{f_j(t)} dt} \leq \bar{X}_{ij}^2(t_{k-1}); \quad (46)$$

at a measurement, $\bar{X}_{ij}^2(t_k)$ is convex in the gain $k(t_k)$, whence:

$$\begin{aligned} \mathbb{E}[\bar{X}_{ij}^2(t_k^+)] &\leq \max(\mathbb{E}[\bar{X}_{ij}^2(t_k^+)], \mathbb{E}[X_{ij}^2(t_k)] + \sigma_{ij}^2(t_k)) \\ &\leq \max(\mathbb{E}[\bar{X}_{ij}^2(t_k^+)], C), \end{aligned} \quad (47)$$

for $C := \frac{\epsilon_i^2 + \epsilon_j^2}{2\alpha} + \Sigma^2$. Both together establish that $\bar{X}_{ij}^2(t)$ is L_2 -bounded. ■

Remark 12 (Gain selection). One option is to pick the gain as $k(t_k) = \min(\frac{\bar{P}_{ij}^-(t_k)}{\bar{P}_{ij}^-(t_k) + \sigma_{ij}^2(t_k)}, \underline{k})$, for some $\underline{k} > 0$, where

$$\frac{d\tilde{P}_{ij}(\tau_j)}{d\tau_j} = \frac{1}{f_j(t)}(-2\alpha\tilde{P}_{ij}(\tau_j) + \epsilon_{ij}^2); \quad \tilde{P}_{ij}^0(0) = 0, \quad (48)$$

$$\Leftrightarrow \frac{d\tilde{P}_{ij}(t)}{dt} = \frac{a_j(t)}{f_j(t)}(-2\alpha\tilde{P}_{ij}(t) + \epsilon_{ij}^2); \quad \tilde{P}_{ij}^0(0) = 0, \quad (49)$$

$$\tilde{P}_{ij}^{t_k^+}(t_k) = \frac{\sigma_{ij}^2(t_k)}{\tilde{P}_{ij}^{t_k^-}(t_k) + \sigma_{ij}^2(t_k)} \tilde{P}_{ij}^{t_k^-}(t_k), \quad (50)$$

The following remark summarizes a discrete version of the optimal filter unconditional error variance.

Remark 13 (Discrete filter). If the filter does not make estimate updates between measurements, then there is no need to run a differential equation, and therefore no implementation issue; it is a discrete Kalman filter. Based on (A-94), its state update equation is

$$X_{ij}(t_{k+1}) = e^{-\alpha(t_{k+1}-t_k)} X_{ij}(t_k) + \Gamma(k) \bar{W}_{ij}(k+1), \quad (51)$$

where $\bar{W}_{ij}(k)$, is a Gaussian white noise sequence and $\Gamma(k) := \frac{\epsilon_{ij}}{\sqrt{2\alpha}} \sqrt{1 - e^{-2\alpha(t_{k+1}-t_k)}}$. Also,

$$\hat{X}_{ij}^{t_{k+1}^-}(t_{k+1}) = e^{-\alpha(t_{k+1}-t_k)} \hat{X}_{ij}^{t_k^+}(t_k), \quad (52)$$

$$P_{ij}^{t_k^-}(t_k) = e^{-2\alpha(t_{k+1}-t_k)} P_{ij}^{t_{k-1}^+}(t_{k-1}) + \Gamma^2(k), \quad (53)$$

$$P_{ij}^{t_k^+}(t_k) = (1 - k(t_k))^2 P_{ij}^{t_k^-}(t_k) + k(t_k)^2 \sigma_{ij}^2(t_k), \quad (54)$$

whence, using an inductive argument,

$$\sup_{t \geq 0} P_{ij}^t(t) \leq \frac{\epsilon_{ij}^2}{2\alpha}. \quad (55)$$

For a practical implementation, we could approximate $t_{k+1} - t_k$ by $\tau_j(t_{k+1}) - \tau_j(t_k)$ if $i, j \neq 0$.

VI. NETWORK-WIDE SMOOTHING OF PAIRWISE ESTIMATES

In this section we make a connection with distributed asynchronous smoothing of pairwise estimates. For illustration, we adopt the asynchronous Jacobi approach of [21]–[23], but other approaches, such as the Randomized Kaczmarz [30], [36], which has showcased better accuracy and energy savings.

We begin the section by presenting a general lemma, and then comment on how this can be used to develop a network-wide offline state estimator. We denote the L^2 -norm by $\|\cdot\|_2$.

Lemma 8 (A generalized least-squares problem). *Given square integrable random vectors $X, Y \in L^2(P)$, where $X \in \mathbb{R}^m$, consider the problem of estimating X by $A^T v$ where $A \in \mathbb{R}^{m \times n}$ is a non-random matrix with (AA^T) invertible, and $v \in \mathbb{R}^n$ is Y -measurable and square-integrable. If the error criterion is $\mathbb{E}[\|X - A^T v\|_2^2 | Y]$, then the unique solution is*

$$v = (AA^T)^{-1} A \mathbb{E}[X|Y], \quad (56)$$

which is the same as solving the deterministic least-squares problem for v with error criterion $\|\mathbb{E}[X|Y] - A^T v\|_2^2$.

Proof: By the orthogonality principle, we have $\mathbb{E}[\|X - A^T v\|_2^2 | Y] = \mathbb{E}[\|X - \mathbb{E}[X|Y]\|_2^2 | Y] + \mathbb{E}[\|\mathbb{E}[X|Y] - A^T v\|_2^2 | Y]$, where the first term is independent of v , and the second one is $\|\mathbb{E}[X|Y] - A^T v\|_2^2$. Minimizing the second term over v yields the result. ■

Let us denote the directed graph of links across which state estimates are available at some given time⁴ by $G = (V, E)$. We assume that the graph is connected. Let us also denote the reduced incidence matrix of the graph [37] obtained from the incidence matrix by removing the row corresponding to node 0, by A . Then AA^T is the principal submatrix of the *Laplacian* of the graph [37], which is known to be positive definite [13] for connected graphs, and hence invertible. Since $X_{ij} = X_j - X_i$ and $X_0 = 0$,

$$X = A^T v, \quad (57)$$

⁴We drop the time indices for ease of notation.

where $X = \{X_{ij}\} \in \mathbb{R}^{|E|}$, $A \in \mathbb{R}^{|E| \times n}$, $v = \{X_i\}_1^n \in \mathbb{R}^n$. Consider now the network-wide estimation problem as one of determining the MMSE estimate v , with error criterion

$$\mathbb{E}[\|X - A^T v\|_2^2 | Y], \quad (58)$$

where $Y := \{y_{ij}\}$ denotes the σ -algebra generated by the measurements obtained till the current time instant, abusing notation and dropping the time indices. The unique solution is $v = (AA^T)^{-1}AE[X|Y]$, which implies that we need to have access to the MMSE estimates of X_{ij} given *all* link measurements. However, because the Brownian motions W_{ij}, W_{kl} are dependent if i or $j \in \{k, l\}$, these MMSE estimators are obtained based on measurements on *at least*⁵ all links adjacent to i, j . Therefore, they are not the same as the pairwise link estimates \hat{X}_{ij} developed in section V, and cannot be used to obtain the MMSE estimate v . A simple fix is to redefine the error criterion, with component-wise conditioning, as

$$\sum_{(i,j) \in E} \mathbb{E}[(X_{ij} - (A^T v)_{ij})^2 | Y_{ij}], \quad (59)$$

whence the MMSE estimate becomes $\bar{v} = (AA^T)^{-1}A\hat{X}$, where $\hat{X} = \{\hat{X}_{ij}\}$. To solve this, we propose using the efficient asynchronous distributed algorithm of [13], [21].

Setting the i -th derivative of $F(v)$ to 0, yields $(AA^T)_i v - A_i \hat{X} = 0$, and a straightforward analysis [13] shows that coordinate descent gives rise to an asynchronous scheme where node i updates its estimate v_i according to

$$v_i = \frac{1}{d_i} \sum_{j:(i,j) \in E \text{ or } (j,i) \in E} (v_j + \hat{X}_{ji}), \quad (60)$$

where d_i , denotes the total degree of node i . Note that the scheme is fully distributed and uses no information about the network topology.

For our problem, spatial smoothing can be used to obtain

- 1) Nodal offset estimates from relative offset estimates since $\tau_{ij} = \tau_j - \tau_i$.
- 2) Nodal skew estimates from relative skew estimates since $\log a_{ij} = \log a_j - \log a_i$.
- 3) Nodal state estimates from relative state estimates since $X_{ij} = X_j - X_i$.

We note in passing that the synchronous version of the exact same scheme [13] can be obtained by using stochastic approximation [38]. In order to solve the system $A^T v - \hat{X} = 0$, or equivalently $AA^T v - A\hat{X} = 0$ we define the stochastic approximation scheme

$$v_{k+1} = v_k - a_k(AA^T v_k - A\hat{X}), \quad (61)$$

⁵In fact the optimal filter derived in section VII shows that they might depend on measurements on *all* links.

since the limiting ODE [38] is $\dot{v}(t) = -AA^T v + A\hat{X}$. In [13], they substitute a_k by a diagonal matrix $D = \text{diag}(\frac{1}{d_1}, \dots, \frac{1}{d_n})$ with entries the inverses of the relative degrees.

VII. NETWORK CLOCK SYNCHRONIZATION

We now develop an asynchronous ⁶ algorithm for the optimal network state estimation problem given by the continuous-discrete Kalman-Bucy filter [12] for the state vector $X_t = \{X_i(t)\} \in \mathbb{R}^n$. We use the convention that all vectors are column vectors. Let us also define node i 's neighborhood $\mathcal{N}_i := \{j \in V : j = i, \text{ or } (i, j) \in E, \text{ or } (j, i) \in E\}$. The following theorem summarizes the optimal continuous-discrete Kalman-Bucy filter equations [12].

Theorem 9 (Network optimal state estimation).

Suppose that nodes $j = 0, \dots, n$ make noisy measurements y_{ij} of X_{ij} over links $(i, j) \in E$, in an asynchronous fashion such that

$$y_{ij}(t_k) = X_{ij}(t_k) + v_{ij}(t_k) = M(t_k)^T X(t_k) + v_{ij}(t_k), \quad (62)$$

where $M(t_k) \in \mathbb{R}^n$, $v_{ij}(t_k) \sim \mathcal{N}(0, \sigma_{ij}^2(t_k))$, and

$$(M(t_k))_m = \begin{cases} -1, & m = i, \\ 1, & m = j, \\ 0, & \text{else.} \end{cases} \quad (63)$$

Then $P_t^t = P_t$, i.e., the conditional and the unconditional covariance coincide. Between measurements, the optimal filter is given by

$$\frac{d\hat{X}_t}{dt} = -\alpha\hat{X}_t, \quad \hat{X}_0 = 0, \quad (64)$$

$$\frac{dP_t}{dt} = -2\alpha P_t + E^2, \quad P_0 = 0_{n \times n}, \quad (65)$$

$$E = \text{diag}(\epsilon_1^2, \dots, \epsilon_n^2). \quad (66)$$

At a measurement, the estimate is updated as follows:

⁶Note that since the goal is to synchronize clocks, a synchronous algorithm can only be implemented in a centralized fashion

$$(\hat{X}_{t_k^+})_m = (\hat{X}_{t_k^-})_m + K(t_k)(y_{ij}(t_k) - \hat{X}_j(t_k^-) + \hat{X}_i(t_k^-)), \quad (67)$$

$$K(t_k) = \frac{P_{mj}^{t_k^-} - P_{mi}^{t_k^-}}{c_k} \quad (68)$$

$$(P^{t_k^+})_{ml} = (P^{t_k^-})_{ml} - \frac{(P_{mj}^{t_k^-} - P_{mi}^{t_k^-})(P_{jl}^{t_k^-} - P_{il}^{t_k^-})}{c_k}, \quad (69)$$

where $c_k := P_{ii}^{t_k^-} + P_{ij}^{t_k^-} - 2P_{ij}^{t_k^-} + \sigma_{ij}^2(t_k)$. It is uniformly asymptotically stable with uniformly bounded covariance.

It is straightforward to extend this scheme to account for the case that two or more measurements are taken at the same time instant t_k .

Nodal skew estimates \hat{a}_i and relative skew estimates \hat{a}_{ij} can be obtained by means of

$$\hat{a}_i(t) = c_i(t)e^{\hat{X}_i(t) + \frac{1}{2}P_{ii}^t(t)}, \quad (70)$$

$$\hat{a}_{ij}(t) = c_{ij}(t)e^{\hat{X}_j(t) - \hat{X}_i(t) + \frac{1}{2}(P_{ii}^t(t) + P_{jj}^t(t) - 2P_{ij}^t(t))}. \quad (71)$$

A. Protocol considerations

The optimal state estimator *cannot* be implemented as is in a decentralized fashion. Except for the implementation issues discussed in Section V-A, (64) and (65) can be implemented in a decentralized fashion such that, for instance, node i updates the state estimate (\hat{X}_t) and the i -th row of the covariance matrix P_t . However, the same is not true at a measurement. In fact, for a connected graph (the situation considered here) *all* entries may be non-zero, which, in turn, implies, cf. (67), (69), that the filter updates at a measurement cannot be run in a decentralized fashion. The rationale for this is as follows: Just before the first measurement, the covariance matrix is diagonal, and after the first measurement, say at link (i, j) , all entries p_{kl} , where k or $l \in i, j$ are updated. Even if we assume that the covariance matrix is local (i.e., $p_{ml} = 0$, if $(m, l) \notin E$) then this won't be necessarily the case after a measurement at link (i, j) since, as is evident from (69), the entry p_{ml} will be updated even if $(m, l) \notin E$, provided that $m, l \in \mathcal{N}_i \cup \mathcal{N}_j$. In particular, nodes that are two hops away will update their corresponding covariance entry. In fact, for a connected graph, there exists a series of measurements after which all entries of the covariance matrix and the state estimator are updated at a measurement in a link.

Therefore, the optimal state estimation algorithm is, by nature, centralized and there would need to be some message passing in order for all nodes to agree on the error covariance matrix which is used in determining the Kalman gains.

Another issue is that relative skew estimates do not have the symmetry property, i.e., $\hat{a}_{ij} \neq \frac{1}{\hat{a}_{ji}}$ in general as is evident from (36); in fact, from (36) and Remark 11, it follows that

$$\hat{a}_{ij}(t)\hat{a}_{ji}(t) = e^{P_{ij}^t(t)} \geq 1. \quad (72)$$

B. A distributed filter for skew estimation

We now describe a distributed suboptimal filter for network-wide estimation of skews. In order to design a distributed algorithm, we impose a constraint on the structure of the gain $K(t_k)$. In particular, on a measurement at link (i, j) , we allow $(K(t_k))_m \neq 0$ only if $m \in \{i, j\}$, which implies the constraint that only the state estimates \hat{X}_i, \hat{X}_j will be updated. Then,

$$P^{t_k^+} = (I - K(t_k)M(t_k)^T)P^{t_k^-}(I - K(t_k)M(t_k)^T)^T + \sigma_{ij}^2(t_k)K(t_k)K(t_k)^T. \quad (73)$$

where $M(t_k)$ is as in (63). The elements of the covariance matrix are updated as follows: If $m, l \notin \{i, j\}$ then $p_{ml}^+ = p_{ml}^-$. If $m \notin \{i, j\}$, then

$$P_{mi}^+ = (1 + k_i)P_{mi}^- - k_i P_{mj}^-, \quad (74)$$

$$P_{mj}^+ = k_j P_{mi}^- + (1 - k_j)P_{mj}^-. \quad (75)$$

Finally

$$P_{ii}^+ = (1 + k_i)((1 + k_i)P_{ii}^- - k_i P_{ij}^-) - k_i((1 + k_i)P_{ij}^- - k_i P_{jj}^-) + k_i^2 \sigma_{ij}^2, \quad (76)$$

$$P_{ij}^+ = (1 + k_i)(k_j P_{ii}^- + (1 - k_j)P_{ij}^-) - k_i(k_j P_{ij}^- + (1 - k_j)P_{jj}^-) + k_i k_j \sigma_{ij}^2, \quad (77)$$

$$P_{jj}^+ = k_j(k_j P_{ii}^- + (1 - k_j)P_{ij}^-) + (1 - k_j)(k_j P_{ij}^- + (1 - k_j)P_{jj}^-) + k_j^2 \sigma_{ij}^2, \quad (78)$$

where k_i, k_j are the i -th and j -th entries of $K(t_k)$. Note that the only diagonal entries of P that are updated are P_{ii}^+, P_{jj}^+ . So minimizing the trace over k_i, k_j boils down to minimizing P_{ii}^+ over k_i , and P_{jj}^+ over k_j . This yields $k_i = -\frac{b_i}{2a}$, $k_j = -\frac{b_j}{2a}$ for

$$a := P_{ii}^- + P_{jj}^- - 2P_{ij}^- + \sigma_{ij}^2 > 0, \quad (79)$$

$$b_i := 2(P_{ii}^- - P_{ij}^-), \quad (80)$$

$$b_j := 2(P_{ij}^- - P_{jj}^-), \quad (81)$$

from which it follows that p_{ii}, p_{jj} decrease at a measurement, i.e.,

$$P_{ii}^+ = -\frac{b_i^2}{4a} + P_{ii}^-, \quad (82)$$

$$P_{jj}^+ = -\frac{b_j^2}{4a} + P_{jj}^-. \quad (83)$$

Remark 14. From (74), it follows that P_{ml} might be updated even if $(m, l) \notin E$, as was the case in the centralized filter. However, this does not constitute a problem for implementation, because the gains depend only on entries of the covariance matrix which are either diagonal or correspond to links.

Remark 15. It follows from (82), that $P_{ii}^+ = \frac{[P_{ii}^-(P_{jj}^- + \sigma_{ij}^2)] - (P_{ij}^-)^2}{(P_{ii}^- + P_{jj}^- + \sigma_{ij}^2) - 2P_{ij}^-}$. If we assume that $P_{ii}^+ \leq \frac{P_{ii}^-(P_{jj}^- + \sigma_{ij}^2)}{P_{ii}^- + P_{jj}^- + \sigma_{ij}^2}$, e.g. if $P_{ij}^- \leq 0$, or $P_{ij}^- \approx 0$ then we are in the setup of Theorem 6 and we can apply the analysis therein to derive variance bounds by substituting Σ^2 by $P_j + \Sigma^2$ where P_j, Σ^2 denote upper bounds on $P_{jj}, \sigma_{ij}^2(t_k)$.

VIII. OFFSET ESTIMATION

We have studied the problem of optimal estimation of the state (logarithms of skews) and the skews. However, clock synchronization ultimately amounts to estimating nodal offsets with respect to a reference clock [2]. Developing a continuous-discrete filter for the estimation of $\tau_i(t) - t$ is problematic because of the dependency of the time displays $\tau_i(t)$ on the skew $a_i(t)$ in (3). Under the assumption of unknown delays, it was shown in [39] that the relative offset between two clocks cannot be estimated unless delays are assumed to be symmetric, or have a known affine characterization of asymmetry [2]. For a link (i, j) , we will assume that delays, as measured in reference clock units, are symmetric. We will use two packets, one sent from node i to node j , and the other sent from node j to node i , together with an estimate of the pairwise skew (as obtained by the pairwise filters in section V) in order to make an estimate of the relative offset $\tau_{ij} := \tau_j - \tau_i$. The estimate can be obtained in a similar way as done in [2], given an estimate of the relative skews $\hat{a}_{ij}(k), \hat{a}_{ji}(k)$ (cf. (14)), by ignoring skew variations between the sent times of the two packets. From Figure 2 and using the notation therein we get:

$$r_{ij}(k) = s_i(k) + \tau_{ij}(t_1) + d_{ij}, \quad (84)$$

$$r_{ji}(k) = s_j(k) + \tau_{ji}(t_3) + d_{ji}, \quad (85)$$

$$\tau_{ij}(t_3) = \tau_{ij}(t_1) + (s_j(k) - r_{ij}(k) + d_{ij})(1 - \hat{a}_{ji}(k)), \quad (86)$$

$$\tau_{ij}(t_4) = \tau_{ij}(t_1) + (r_{ji}(k) - s_i(k))(\hat{a}_{ij}(k) - 1), \quad (87)$$

where d_{ij}, d_{ji} are the delays as measured by the local clocks, j, i respectively. Using $\tau_{ji}(t_3) = -\tau_{ij}(t_3)$ and $d_{ij} = \hat{a}_{ij}d_{ji}$ we get:

$$\hat{\tau}_{ij}(k) = -r_{ji}^{(k)} + (s_j^{(k)} + \hat{a}_{ij}\hat{d}_{ji}), \quad (88)$$

$$\hat{d}_{ij}(k) := \frac{1}{2\hat{a}_{ij}}[(r_{ji}^{(k)} - s_j^{(k)}) + (r_{ij}^{(k)} - s_i^{(k)}) + (s_j^{(k)} - r_{ij}^{(k)})(1 - \hat{a}_{ji})]. \quad (89)$$

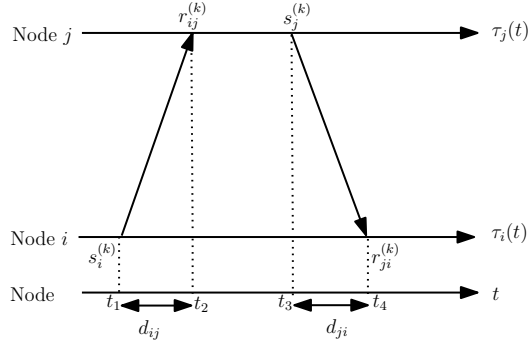


Fig. 2. Message exchanges between two nodes for offset estimation

An analysis of (88) based on stochastic Taylor approximation carried out in a similar way as was done in section IV, so as to bound the approximation error.

Using this scheme, pairwise estimates of the relative offsets can be obtained. Then, the spatial smoothing algorithm [13], [21] presented in section VI can be used for the offline smoothing of the pairwise estimates, since relative offsets also satisfy constraints of the form $\tau_{ij} = \tau_j - \tau_i$.

A. Performance evaluation of clock synchronization algorithms

Because of link delays, it is impossible for a node to have instantaneous access to another node's clock display, and we need the scheme of the previous section to estimate relative offsets. The relative offset estimates cannot be used as a practical metric for clock synchronization performance. A metric of performance can be derived based on the fact that (cf. Figure 1)

$$\bar{a}_{ij}(t_k) = \left| \frac{r_{i,j}^{(k+1)} - r_{i,j}^{(k)}}{s_i^{(k+1)} - s_i^{(k)}} \right|, \quad (90)$$

if the link delays of the two packets (as measured in clock i 's units) are assumed to be the same constant. We use the $\bar{a}_{ij}(t_k)$ to denote the average relative skew in the interval $[s_i^{(k)}, s_i^{(k+1)}]$ of clock i . Node i can predict the receipt time of the second packet, $s_i^{(k+1)}$, using $s_i^{(k)}, r_{i,j}^{(k)}, s_i^{(k+1)}$ and an estimate of $\bar{a}_{ij}(t_k)$. This can be then compared to the actual receipt time to obtain a metric of clock synchronization.

IX. MODEL-BASED CLOCK SYNCHRONIZATION PROTOCOL (MBCSP)

In this section, we combine our previous analysis to present the specifications of a proposed model-based distributed clock synchronization protocol. We consider the same abstraction regarding the network topology as in Section VII.

Nodes can exchange time-stamped packets with their neighbors in an asynchronous fashion. We consider two modes of communication:

- 1) **Skew estimation:** A node i sends two packets with minimal time separation to a neighboring node j as explained in Section IV and depicted in Figure 1. Node i includes its parameter ϵ_i in the second packet sent to node j , along with its state estimate \hat{X}_i and p_{ii}, p_{ij} .
- 2) **Offset estimation:** A node i sends a packets to node j . Upon receipt, node j sends a packet to node i . Node i includes its parameter ϵ_i , along with its state estimate \hat{X}_i and p_{ii}, p_{ij} in the first packet sent to node j . This is depicted in Figure 2.

In both modes, the sending node time-stamps and includes in the packet the time (according to its local clock) that it sends a packet while the receiving node time-stamps the time (according to its local clock) that it receives a packet.

An arbitrary node in the network, say node i , is required to store parameters α, ϵ_i , as well as

- (i) Its state estimate \hat{X}_i .
- (ii) The i -th row of the covariance matrix, $\{P_{ij}\}_{j=1}^n$.
- (iii) Its nodal offset estimate $\widehat{\tau_i - t}$.
- (iv) For any neighboring node, say node j , the relative offset estimate $\hat{\tau}_{ij}$.
- (v) The last time, according to its local clock, that it performed a state estimate update (along with an update of the i -th row of the covariance matrix), based on either (64), (65) or (67) and the covariance update equations of Section VII-B. We denote this time by u_i .

Each node, is responsible for calling four routines:

- 1) **Skew update:** Upon receipt of the second packet in the *skew estimation* mode, say from node i to node j (see Figure 1), node j has all four time-stamps $s_i^{(k)}, s_i^{(k+1)}, r_{i,j}^{(k)}, r_{i,j}^{(k+1)}$, as well as $\alpha, \epsilon_i, \epsilon_j$. Node j makes a measurement according to (28); if node i is node 0 then $t_k = s_i^{(k)}$, otherwise $r_{i,j}^{(k+1)}$ can be used instead. Before node i sends the second packet, it updates its state estimate along with the i -th row of the covariance matrix according to

$$\hat{X}_i^{t_{k+1}^-} = e^{-\alpha \Delta t_k} \hat{X}_i^{t_k^+}(t_k), \quad (91)$$

$$P_{ij}^{t_k^-}(t_k) = e^{-2\alpha \Delta t_k} P_{ij}^{t_{k-1}^+}(t_{k-1}) + \frac{\epsilon_j^2}{2\alpha} (1 - e^{-2\alpha \Delta t_k}) \mathbb{I}_{j=i}, \quad (92)$$

where \mathbb{I} denotes the characteristic, function and $\Delta t_k := t_{k+1} - t_k$; it can be approximated by the difference $s_i^{(k+1)} - u_i$. Node i includes its updated state \hat{X}_i as well as the updated values for P_{ii}, P_{ij} . Finally, node i sets $u_i = s_i^{(k+1)}$. Upon receipt of the second packet, node j updates its state estimate

along with the j -th row of the covariance matrix according to (91), (92) where now Δt_k can be approximated with $r_{i,j}^{(k+1)} - u_j$, and then u_j is updated to $r_{i,j}^{(k+1)}$. Then, node j calculates the state and covariance updates after the measurement based on (67), along with the covariance update equations of Section VII-B. Node j can send an ACK packet to node i and i performs the exact same tasks as j .

- 2) **Relative offset update:** Before the sender, say node i , sends the first packet in the *offset estimation* mode to a receiver, say node j , (see Figure 2), node i updates its state estimate \hat{X}_i and the i -th row of the covariance matrix according to (91), (92) where now Δt_k can be approximated with $s_i^{(k)} - u_i$, and then u_i is updated to $s_i^{(k)}$. Node i includes in this packet $\hat{X}_i, P_{ii}, P_{ij}$. Upon receipt of this packet, node j also updates its state estimate \hat{X}_j and the j -th row of the covariance matrix according to (91), (92) where now Δt_k can be approximated with $r_{i,j}^{(k)} - u_j$, and then u_j is updated to $r_{i,j}^{(k)}$. Then, node j can estimate $\hat{a}_{ij}, \hat{a}_{ji}$ based on (71), where t is approximated by $s_i^{(k)}$ and $r_{i,j}^{(k)}$, respectively. A symmetric estimate can then be calculated by $\hat{a}_{ij} \leftarrow \sqrt{\frac{\hat{a}_{ij}}{\hat{a}_{ji}}}$, and $\hat{a}_{ji} = \frac{1}{\hat{a}_{ij}}$.

Upon receipt of the second packet in the *offset estimation* mode, from node j to node i (see Figure 2), node i has all four time-stamps $s_i^{(k)}, r_{i,j}^{(k)}, s_j^{(k)}, r_{j,i}^{(k)}$ along with the estimate \hat{a}_{ij} , so it can perform offset and delay estimation according to (88) and (89). The delay estimate needs to be non-negative so we set $\hat{d}_{ij} = \max(\hat{d}_{ij}, 0)$, and $\hat{d}_{ji} = \hat{a}_{ij}\hat{d}_{ij}$. Node i can send an ACK packet to node j in order to agree on an estimate $\hat{\tau}_{ji}(k) = -\hat{\tau}_{ij}(k)$.

- 3) **Spatial smoothing:** Upon the completion of the *relative offset update*, nodes i and j perform a spatial smoothing update based on (60) where v_i represents $\widehat{\tau_i - t}$ and \hat{X}_{ji} represents $\hat{\tau}_{ji}$.
- 4) **Time prediction:** Upon completion of the *skew update* task (after the receipt of the second packet in the *skew estimation* mode, say from node i to node j (see Figure 1)) node i can compute the predicted receipt time of the second packet, $r_{i,j}^{(k+1)}$, if the ACK packet contains $r_{i,j}^{(k+1)}$ based on the discussion in Section VIII-A. This requires a calculation of \hat{a}_{ij} , which can be performed in the exact same way as was done in *relative offset update*. Node i can then obtain the difference of the predicted receipt time to the actual value $r_{i,j}^{(k+1)}$. The same difference is computable by node j .

We refer to this protocol as Model-based Clock synchronization protocol (MBCSP). We have implemented MBCSP in Matlab with the graph abstraction for the network topology (cf. Section IV). In order to make the scenario realistic with the interference in wireless networks, we have also implemented a simple Medium Access Control (MAC) [6] mechanism, where two interfering transmissions collide and packets get dropped. Without serious loss of generality, we use the primary interference model [6], in

which a node cannot be transmitting a packet to more than one node and cannot be receiving a packet by more than one node. In addition, a node is not allowed to be transmitting if it is receiving a packet. These constraints require the activation set, defined as the set of links activated at each time, to be a matching [37].

We test MBCSP against the protocol of [21], which will be hereafter referred to as Spatial Smoothing (SS). In this protocol, relative skews are calculated based on only link relative skew measurements using exponential forgetting. Nodal skew estimates are obtained using spatial smoothing as explained in Section VI. Relative offset estimates are obtained using the formulas in Section VIII, and are consequently smoothed using spatial smoothing to obtain nodal offset estimates.

We have also implemented a protocol that performs relative skew estimation using the pairwise filter of Section V instead of the distributed network filter of Section VII-B. Nodal skew estimation is accomplished using the spatial-smoothing algorithm (cf. Section VI) while offset estimation is carried out in the exact same way as MBCSP. We refer to this as *Hybrid* protocol. Its performance is intuitively expected to lie in between that of SS and MBCSP, which we validate in the next section.

X. SIMULATIONS

we present simulation results of the model properties and the performance of the clock synchronization protocol.

In Figure 3 we present a simulation of the skew and time display of a clock with $\alpha_i = 10, \epsilon_i = 1$ for 30 reference time units, using Matlab. The fluctuations in the instantaneous skew give rise to a time-varying offset.

In Figure 3 we present a simulation of the clock display variance (cf. (A-103)) and its lower bound (cf. (A-106)) for two different clocks, with parameters $\alpha_i = 10, \epsilon_i = 1$ and $\alpha_i = 10, \epsilon_i = 10$ for 20 reference time units. The upper bound (cf. (A-105)) is not displayed because it appears to vastly overestimate the variance. Both the variance and its lower bound appear to grow *linearly* with time; in fact we applied a curve-fitting approach with a nominal curve ax^b , and the exponent was estimated close to 1 in both cases with small mean-square error (MSE).

In Figure 5 we illustrate the Allan variance of a clock with the same parameters as above and a comparison with the performance index of Remark 8. Unlike the index of Remark 8, the Allan variance is not an increasing function. However, the approximation is good for small values of T .

In Figure 6, we present the measured Allan variance for a Berkeley mote clock [21], as well as the best fit for the Allan variance of our model (26 using Matlab; the parameters corresponding to the best

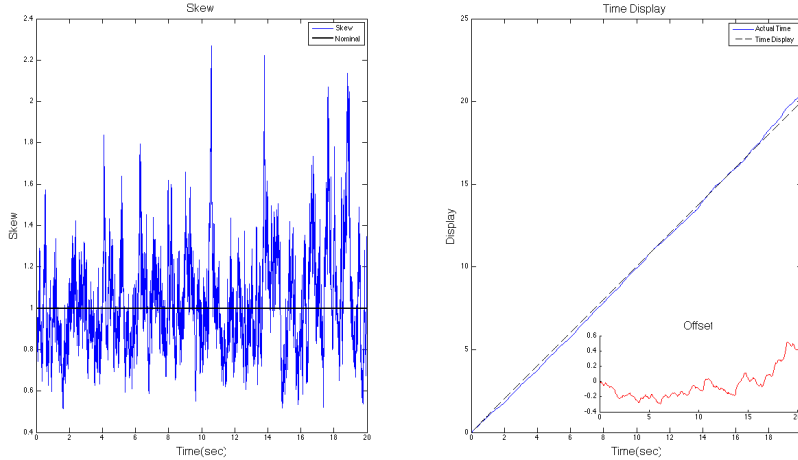


Fig. 3. Instantaneous skew and time display for a clock with $\frac{\alpha_i}{\epsilon_i} = 10$.

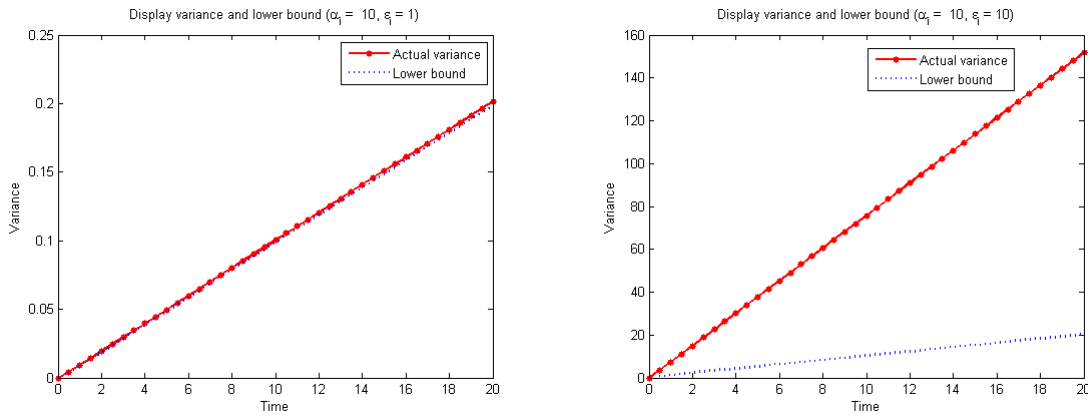


Fig. 4. Display variance and lower bound for two different clocks.

fit were $\hat{\alpha}_i = 66.4, \hat{\epsilon}_i = 4.15 \cdot 10^{-5}$. It is evident that the model can only capture a decay of the Allan variance with τ but is unable to capture the fact that Allan variance appears to increase for $\tau \geq 60s$. However, note that the scale is logarithmic and the average absolute error of the fit is $4.4659 \cdot 10^{-10}$.

We have studied the performance degradation of the distributed filter of Section VII-B as opposed to the optimal centralized Kalman filter (cf. Section VII) for various network topologies. In all cases, the variance of the suboptimal filter was very close to the optimal variance. In Figure 7, we present the average state variance (trace of the covariance measurement divided by the size of the state) for a linear network with 10 clocks with parameters $\alpha = 10, \epsilon = 1$. Measurements are taken every $T = 0.002$ times

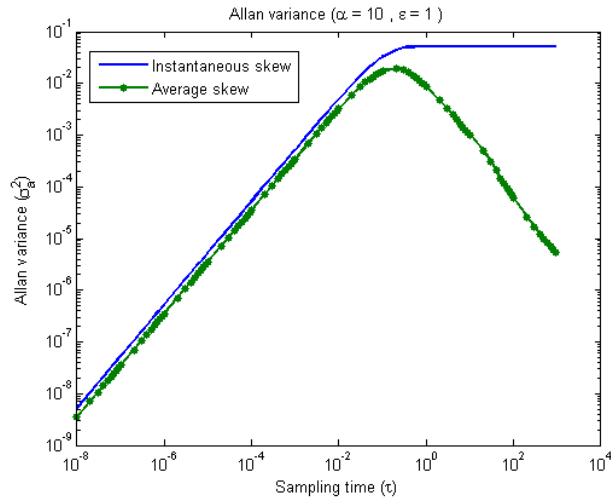


Fig. 5. Allan variance vs asymptotic skew difference variance for a clock with $\frac{\alpha_i}{\epsilon_i} = 10$.

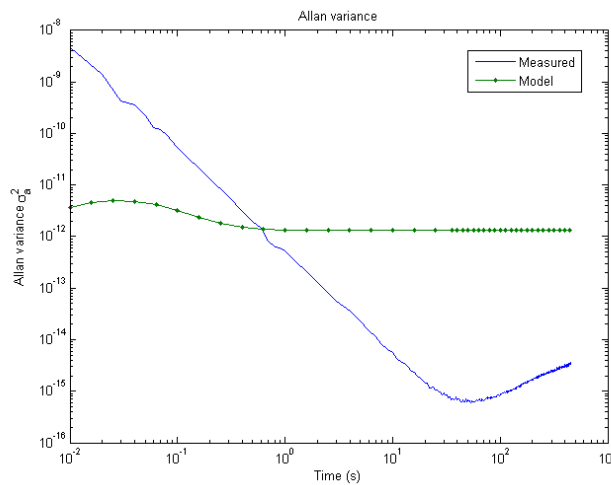


Fig. 6. Parameter estimation using Allan variance.

units, and for each measurement, one link is selected at random. The performance degradation is defined as the ratio of the distributed filter variance to the variance of the optimal Kalman filter.

We have simulated the performance of MBCSP against both SS [21] and the Hybrid scheme defined in the previous section. The results in Figure 8 were obtained for 2 clocks and 5 clocks respectively. The clock parameters are set to $\alpha = 10, \epsilon = 1$. The time precision, i.e., the sampling time of the numerical simulation (cf. remark 3), is set to $\Delta t = 10^{-5}$. Delays are generated as random variables independent,

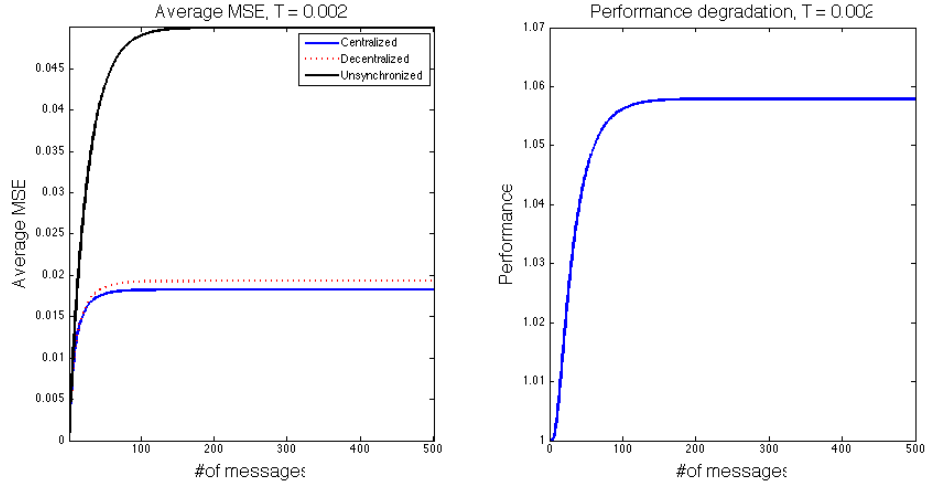


Fig. 7. Performance degradation of distributed state estimation filter for a linear network with 10 nodes and random periodic measurements.

uniformly distributed with mean $500\Delta t$. For skew estimation, the two packets of Figure 1 are sent with a separation of $40\Delta t$, while the second packet for offset estimation (cf. Figure 2) is sent $20\Delta t$ after the first one is received. Measurements are performed at random times and random links with frequency $1/|E|$ for skew estimation, and $6/|E|$ for offset estimation, where the unit time is defined as $\frac{1}{\Delta t}$ mini-slots, and $|E|$ is the number of directed links in the network. We have conducted the simulations for 120 time units and different realizations of the white noises. The results of Figure 8 illustrate mean absolute errors (MAE); we use three indices, namely the nodal skew estimation MAE, nodal offset estimation MAE, and the MAE in predicting receipt times (cf. Section VIII-A). The columns labeled as “No sync” are used to present the mean absolute real values of the corresponding quantities.

We have performed numerous simulations for various parameters and network topologies. In all cases, we observed that Hybrid and MBCSP track the clock skews significantly better than the ad-hoc exponential forgetting scheme of SS. This results in more accurate relative offset estimates, delay estimates predicted receipt times. However, since both schemes use the Spatial Smoothing algorithm (cf. Section VI) to obtain nodal offset estimates from relative offset estimates, their accuracy in nodal offset estimates is comparable. We also observed that the Hybrid scheme performs significantly better than SS but worse than MBCSP⁷.

⁷Note that in the case of only two nodes (pairwise synchronization) the offset estimation accuracy is, trivially, the same.

Node	Offset				Skew				Prediction		
	No sync	SS	Hybrid	MBCSP	No sync	SS	Hybrid	MBCSP	SS	Hybrid	MBCSP
1	0.00000	0.00000	0.00000	0.00000	1.00000	0.00000	0.00000	0.00000	0.01657	0.01359	0.01364
2	0.57687	0.00131	0.00120	0.00119	1.00548	0.20866	0.16970	0.17014	0.01657	0.01359	0.01364

Node	Offset				Skew				Prediction		
	No sync	SS	Hybrid	MBCSP	No sync	SS	Hybrid	MBCSP	SS	Hybrid	MBCSP
1	0.00000	0.00000	0.00000	0.00000	1.00000	0.00000	0.00000	0.00000	0.04115	0.02609	0.02655
2	0.60233	0.02310	0.02308	0.02307	1.02628	0.21036	0.18741	0.17734	0.04113	0.02610	0.02656
3	0.29349	0.02044	0.02038	0.02038	1.01466	0.22604	0.17117	0.16513	0.04111	0.02609	0.02655
4	1.71270	0.02049	0.02043	0.02043	0.98548	0.21835	0.16800	0.16808	0.04111	0.02610	0.02654
5	0.48743	0.02193	0.02193	0.02191	1.00192	0.21063	0.16870	0.16165	0.04115	0.02609	0.02654

Fig. 8. Performance evaluation of clock synchronization algorithms based on data obtained from MATLAB simulations.

We have obtained real clock data from two Berkeley motes [21] exchanging time-stamps in the two communication modes described in Section IX, namely skew and offset estimation. Based on the time-stamp collection we performed a trace-driven simulation⁸ to obtain a comparative evaluation of the three schemes. Clock parameters α_2, ϵ_2 were estimated based on Allan variance, as shown above, to be $\hat{\alpha}_i = 66.4, \hat{\epsilon}_i = 4.15 \cdot 10^{-5}$. The accuracy was set to $1\mu s$. The results are presented in Figure 9. In this case, we cannot define the real skews and offsets so we present the offset and skew estimates obtained from the three different schemes, in mean absolute value. However, we can still define the prediction MAE which is the metric of performance for clock synchronization algorithms (cf. Section VIII-A). The prediction MAE is very low in all cases, in the order of tens of μs , which means that the receipt times are precisely predicted within the clock accuracy of $1\mu s$ in many cases. Our schemes yield a 45% decrease in the prediction MAE.

Node	Offset			Skew			Prediction		
	SS	Hybrid	MBCSP	SS	Hybrid	MBCSP	SS	Hybrid	MBCSP
1	0.00000	0.00000	0.00000	1.00000	1.00000	1.00000	6.74515e-07	3.84218e-07	3.84218e-07
2	453.82502	453.82502	453.82502	0.99996	1.00000	1.00000	6.74599e-07	3.84207e-07	3.842070e-07

Fig. 9. Trace-driven simulation of clock synchronization algorithms based on data obtained from Berkeley motes.

⁸Note that trace-driven simulation is equivalent to an actual implementation, since our protocols use only the acquired time-stamps and have minimal computational complexity.

XI. CONCLUSION

We have developed a mathematical model for the skews and the time displays of different clocks and analyzed its properties. The instantaneous skews given by the model have expected value 1 at all times, while their variance is bounded. Additionally, time displays are unbiased, but, nonetheless, their variance grows with time, which makes the synchronization problem challenging. We have calculated the Allan variance [11] of the model. It was shown that if a different clock is taken as reference, the time displays of all other clocks can be expressed with respect to it using the same model, with different parameters and a change of time scales. We have developed and analyzed a method to obtain noisy state measurements on a link, and used these measurements to develop a continuous-discrete Kalman-Bucy filter for the pairwise estimation of the logarithm of skews. The differential equations of the pairwise estimator are not readily implementable since they require integration with respect to the unknown reference time, so we have proposed an implementable stable filter which has uniform bounded unconditional variance. The analysis of the pairwise estimation was applied to handle the network-wide state estimation in three ways. First, an off-line algorithm for the filtering of pairwise estimates was proposed, and it was shown that using the distributed scheme of [21], [13] for the smoothing of pairwise estimates is optimal for a particular selection of error criterion. In addition, the optimal linear filtering equations were derived for the network case, which give rise to an online asynchronous centralized scheme which is stable and of bounded variance. We have also described an efficient distributed suboptimal scheme. Finally, we have presented a scheme to estimate relative offset estimates based on estimates of the relative skews, and suggested the spatial smoothing algorithm of [21] to obtain nodal offset estimates from relative offset estimates. We have implemented our protocol in Matlab and have conducted a simulation study that shows increase of performance compared to [21] for the model under study. We have also performed trace-driven simulation based on time-stamps obtained by Berkeley motes. Our scheme outperforms the one in [21] by 45%, where we used the accuracy in predicting receipt time-stamps as synchronization metric.

REFERENCES

- [1] N. Freris, H. Kowshik, and P. R. Kumar, "Fundamentals of Large Sensor Networks: Connectivity, Capacity, Clocks and Computation," *Proceedings of the IEEE*, vol. 98, no. 1, pp. 1828–1846, Nov. 2010.
- [2] N. Freris, S. Graham, and P. R. Kumar, "Fundamental Limits on Synchronizing Clocks over Networks," *IEEE Transactions on Automatic Control*, vol. 56, no. 4, pp. 1352–1364, Jun. 2011.
- [3] Q. Li and D. Rus, "Global clock synchronization in sensor networks," *IEEE Transactions on Computers*, vol. 55, pp. 214–226, 2006.

- [4] S. Graham and P. R. Kumar, "The Convergence of Control, Communication, and Computation," in *Proceedings of Personal Wireless Communication*. Heidelberg: Springer-Verlag, Oct. 2003, pp. 458–475.
- [5] K. Plarre and P. R. Kumar, "Tracking objects with networked scattered directional sensors," *EURASIP Journal on Advances in Signal Processing*, vol. 2008, 2008, article ID: 360912, 10 pages.
- [6] R. McCabe, N. Freris, and P. R. Kumar, "Controlled Random Access MAC for Network Utility Maximization in Wireless Networks," in *Proceedings of the 47th IEEE Conference on Decision and Control*, Cancun, Dec. 2008, pp. 2350–2355.
- [7] F. Sivrikaya and B. Yener, "Time Synchronization in Sensor Networks: a survey," *IEEE Network*, vol. 18, no. 4, pp. 45–50, Jul.-Aug. 2004.
- [8] S. Ganeriwal, R. Kumar, and M. Srivastava, "Timing-Sync Protocol for Sensor Networks," in *Proceedings of the 1st Conference on Embedded Networked Sensor System (SenSys)*. ACM, Nov. 2003, pp. 138–149.
- [9] N. Freris, V. Borkar, and P. R. Kumar, "A model-based approach to clock synchronization," in *Proceedings of the 48th IEEE Conference on Decision and Control*, Sanghai, Dec. 2009, pp. 5744–5749.
- [10] D. Veitch, S. Babu, and A. Pasztor, "Robust Synchronization of Software Clocks across the Internet," in *Proceedings of the 4th SIGCOMM conference on Internet measurement*. Sicily: ACM, Oct. 2004, pp. 25–27.
- [11] D. W. Allan, "Time and frequency (time-domain) characterization, estimation, and prediction of precision clocks and oscillators," *IEEE Transactions on Ultrasonics, Ferroelectrics, and Frequency Control*, vol. 34, pp. 647–654, Nov. 1987.
- [12] A. Jazwinski, *Stochastic Processes and Filtering Theory*. New York: Academic Press, 1970.
- [13] A. Giridhar and P. R. Kumar, "Distributed Clock Synchronization over Wireless Networks: Algorithms and Analysis," in *Proceedings of the 45th IEEE Conference on Decision and Control*, San Diego, Dec. 2006, pp. 4915–4920.
- [14] P. Barooah and J. Hespanha, "Distributed Estimation from Relative Measurements in Sensor Networks," in *Proceedings of the 2nd International Conference on Intelligent Sensing and Information Processing*, Dec. 2005, pp. 226–231.
- [15] B. Sundararaman, U. Buy, and A. Kshemkalyani, "Clock Synchronization for Wireless Sensor Networks: a survey," *Ad Hoc Networks*, vol. 3, pp. 281–323, May 2005.
- [16] B. Sadler and A. Swami, "Synchronization in Sensor Networks: an overview," in *Military Communications Conference (MILCOM)*. IEEE, Oct. 2006, pp. 1–6.
- [17] D. L. Mills, "Internet Time Synchronization: the Network Time Protocol," *IEEE Transactions on Communications*, vol. 39, no. 10, pp. 1482–1493, Oct. 1991.
- [18] J. Elson, L. Girod, and D. Estrin, "Fine-Grained Network Time Synchronization using Reference Broadcasts," in *Proceedings of the 5th Symposium on Operating Systems Design and Implementation*, Boston, MA, Dec. 2002, pp. 147–163.
- [19] M. Maroti, G. Simon, B. Kusy, and A. Ledeczi, "The Flooding Time Synchronization Protocol," in *Proceedings of the 2nd International Conference on Embedded Networked Sensor Systems*, Baltimore, Nov. 2004, pp. 39–49.
- [20] J. Elson, R. Karp, C. H. Papadimitriou, and S. Shenker, "Global Synchronization in Sensornets," in *Proceedings of LATIN*. Buenos Aires: Springer, 2004, pp. 609–624.
- [21] R. Solis, V. Borkar, and P. R. Kumar, "A New Distributed Time Synchronization Protocol for Multihop Wireless Networks," in *Proceedings of the 45th IEEE Conference on Decision and Control*, San Diego, Dec. 2006, pp. 2734–2739.
- [22] A. Giridhar and P. R. Kumar, "The Spatial Smoothing Method of Clock Synchronization in Wireless Networks," *Theoretical Aspects of Distributed Computing in Sensor Networks*, pp. 227–256, 2011.
- [23] P. Barooah, N. da Silva, and J. Hespanha, "Distributed Optimal Estimation from Relative Measurements for Localization and Time Synchronization," *Distributed Computing in Sensor Systems, Lecture Notes in Computer Science*, vol. 4026, pp. 266–281, Jun. 2006.

- [24] P. Barooah and J. Hespanha, “Error Scaling Laws for Optimal Estimation from Relative Measurements,” *IEEE Transactions on Information Theory*, vol. 55, no. 12, pp. 5661–5673, Dec. 2009.
- [25] P. Barooah, J. Hespanha, and A. Swami, “On the effect of Asymmetric Communication on Distributed Time Synchronization,” in *Proceedings of the 46th IEEE Conference on Decision and Control*, New Orleans, LA, Dec. 2007, pp. 5465–5471.
- [26] C. Liao and P. Barooah, “Time Synchronization in Mobile Sensor Networks from Relative Measurements,” in *Proceedings of the 49th IEEE Conference on Decision and Control*, Atlanta, GA, Dec. 2010, pp. 2118–2123.
- [27] P. Barooah and J. Hespanha, “Estimation on Graphs from Relative Measurements,” *IEEE Control Systems Magazine*, vol. 27, no. 4, pp. 57–74, Aug. 2007.
- [28] O. Simeone and U. Spagnolini, “Distributed time synchronization in wireless sensor networks with coupled discrete-time oscillators,” *EURASIP Journal on Wireless Communications and Networking*, vol. 2007, 2007, article ID: 57054, 13 pages.
- [29] J. He, P. Cheng, L. Shi, and J. Chen, “Time synchronization in WSNs: A maximum-value-based consensus approach,” *IEEE Transactions on Automatic Control*, vol. PP, no. 99, pp. 1–1, 2013.
- [30] N. Freris and A. Zouzias, “Fast distributed smoothing of relative measurements,” in *51st IEEE Conference on Decision and Control*, Maui, Dec. 2013, pp. 1411–1416.
- [31] L. Galleani, L. Sacerdote, P. Tavella, and C. Zucca, “A mathematical model for the atomic clock error,” *Metrologia*, vol. 40, pp. 257–264, 2003.
- [32] J. W. Chaffee, “Relating the Allan variance to the diffusion coefficients of a linear stochastic differential equation model for precision oscillators,” *IEEE Transactions on Ultrasonics, Ferroelectrics, and Frequency Control*, vol. 34, pp. 655–658, Nov. 1987.
- [33] D. Revuz and M. Yor, *Continuous Martingales and Brownian Motion*. Springer, 2001.
- [34] P. Kloeden and E. Platen, *Numerical solution of stochastic differential equations*. Springer-Verlag, 2009.
- [35] D. Stroock, *Probability Theory: An Analytic View*. Cambridge, MA: Cambridge University Press, 1993.
- [36] A. Zouzias and N. Freris, “Randomized Extended Kaczmarz for solving Least Squares,” *SIAM Journal on Matrix Analysis and Applications*, vol. 34, no. 2, pp. 773–793, 2013.
- [37] D. West, *Introduction to Graph Theory*. Englewood Cliffs, NJ: Prentice Hall, 1996.
- [38] V. Borkar, *Stochastic Approximation: A Dynamical System Viewpoint*. New Delhi and Cambridge, UK: Hindustan Publishing Agency and Cambridge University Press, 2008.
- [39] S. Graham and P. R. Kumar, “Time in General-purpose Control Systems: The Control Time Protocol and an experimental evaluation,” in *Proceedings of the 43rd IEEE Conference on Decision and Control*, Bahamas, Dec. 2004, pp. 4004–4009.
- [40] H. Royden, *Real Analysis*. Stanford, CA: Prentice Hall, 1988.

APPENDIX A

PROOF OF LEMMA 1

By applying Itô’s formula [12] to the function $f(X_i(t), t) := X_i(t)e^{\alpha_i t}$ we have

$$df(X_i(t), t) = \epsilon_i e^{\alpha_i t} dW_i(t). \quad (\text{A-93})$$

Hence, the solution of (1) satisfies

$$X_i(t) = \epsilon_i \int_0^t e^{-\alpha_i(t-s)} dW_i(s), \quad (\text{A-94})$$

which, in turn, shows that $X_i(t)$ is a zero-mean Gaussian random variable. The variance can be computed by use of Itô's isometry [12]:

$$\mathbb{E}[X_i(t)^2] = \epsilon_i^2 \int_0^t e^{-2\alpha_i(t-s)} ds = \frac{\epsilon_i^2}{2\alpha_i} (1 - e^{-2\alpha_i t}). \quad (\text{A-95})$$

This further implies that

$$\mathbb{E}[a_i(t)] = \mathbb{E}[e^{X_i(t)}] e^{-\frac{1}{4} \frac{\epsilon_i^2}{\alpha_i} (1 - e^{-2\alpha_i t})} = 1, \quad (\text{A-96})$$

$$\begin{aligned} \text{Var}(a_i(t)) &= c_i^2(t) \mathbb{E}[e^{2X_i(t)}] - 1 \\ &= e^{\frac{\epsilon_i^2}{2\alpha_i} (1 - e^{-2\alpha_i t})} - 1 \nearrow e^{\frac{\epsilon_i^2}{2\alpha_i}} - 1. \end{aligned} \quad (\text{A-97})$$

By Tonelli's theorem [40]

$$\mathbb{E}[\tau_i(t)] = \int_0^t \mathbb{E}[a_i(t')] dt' = t. \quad (\text{A-98})$$

It follows from (A-94) and Tonelli's theorem that

$$\text{Var}(\tau_i(t)) = \int_0^t \int_0^t \mathbb{E}[a_i(r)a_i(s)] ds dr - t^2. \quad (\text{A-99})$$

Note that $\mathbb{E}[a_i(r)a_i(s)] = c_i(r, s) \mathbb{E}[e^{X_i(r)+X_i(s)}]$, where $c_i(r, s) := e^{-\frac{\epsilon_i^2}{4\alpha_i} (2 - e^{-2\alpha_i r} - e^{-2\alpha_i s})}$ and $X_i(r) + X_i(s) \sim \mathcal{N}(0, \sigma_i^2(r, s))$ with $\sigma_i^2(r, s) := -2 \log c_i(r, s) + 2\mathbb{E}[X_i(r)X_i(s)]$. From (A-94) and Itô's isometry we have

$$\mathbb{E}[X_i(r)X_i(s)] = \epsilon_i^2 e^{-\alpha_i(r+s)} \mathbb{E}\left[\int_0^r e^{\alpha_i t} dW_i(t) \int_0^s e^{\alpha_i t} dW_i(t)\right] \quad (\text{A-100})$$

$$= \epsilon_i^2 e^{-\alpha_i(r+s)} \int_0^{s \wedge r} e^{2\alpha_i t} dt = \frac{\epsilon_i^2}{2\alpha_i} e^{-\alpha_i(r+s)} (e^{2\alpha_i s \wedge r} - 1), \quad (\text{A-101})$$

where $a \wedge b := \min(a, b)$. Therefore

$$\mathbb{E}[a_i(r)a_i(s)] = e^{\frac{\epsilon_i^2}{2\alpha_i} e^{-\alpha_i(r+s)} (e^{2\alpha_i s \wedge r} - 1)}, \quad (\text{A-102})$$

which, in turn, yields

$$\text{Var}(\tau_i(t)) = 2 \int_0^t \int_0^r e^{f(s,r)} ds dr - t^2, \quad (\text{A-103})$$

$$\text{where } f(s, r) := \frac{\epsilon_i^2}{2\alpha_i} e^{-\alpha_i r} (e^{\alpha_i s} - e^{-\alpha_i s}). \quad (\text{A-104})$$

Evaluating the integral (A-103) analytically is not possible, so we study the asymptotic behavior of the variance. For $r \leq s$, $f(s, r)$ is strictly decreasing in r , and strictly increasing in s , therefore $f(s, r) \leq f(s, s)$. Also note that $g(s) := f(s, s)$ is strictly increasing. This implies that

$$\text{Var}(\tau_i(t)) < (e^{\frac{\epsilon_i^2}{2\alpha_i}} - 1)t^2 = O(t^2). \quad (\text{A-105})$$

To obtain a lower bound on $Var(\tau_i(t))$ we use Jensen's inequality [40] to get

$$Var(\tau_i(t)) \geq (A - 1)t^2, \quad (\text{A-106})$$

$$A := e^{\frac{2}{i^2} \int_0^t \int_0^r f(s,r) ds dr} = e^{h(t)},$$

$$h(t) := \frac{1}{t^2} \frac{\epsilon_i^2}{\alpha_i^2} \left(t + \frac{1}{2\alpha_i} (1 - e^{-2\alpha_i t}) - \frac{2}{\alpha_i} (1 - e^{-\alpha_i t}) \right) = \Omega(1/t).$$

The rest follows from $(e^{\Omega(\frac{1}{t})} - 1)t^2 = \Omega(t)$. ■

APPENDIX B

PROOF OF THEOREM 5

Definition 1. For stochastic variables, $y(t), x(t)$ depending on a parameter t , whenever we write $y(t) = x(t) + O(t^k)$, for some real number k , this is interpreted in the L^2 -norm, that is to say there exists a $c > 0$, such that $\mathbb{E}[(y(t) - x(t))^2] \leq ct^{2k}$, for all $t \in (0, 1)$, in particular $\overline{\lim}_{t \rightarrow 0^+} \frac{\mathbb{E}[(y(t) - x(t))^2]^{\frac{1}{2}}}{t^k} < \infty$. The extensions for $\Theta(\cdot), \Omega(\cdot), o(\cdot)$ and for the vector case are straightforward.

An application of Cauchy-Schwartz inequality [40] yields that $O(t^k)O(t^l) = O(t^{k+l})$, while Minkowski's inequality [40] yields $O(t^k) + O(t^l) = O(t^{k \wedge l})$. The following result shows how to perform a first-order stochastic Taylor expansion for the processes under study, namely, skews and time displays.

Lemma 10 (Stochastic Taylor's expansion). *For $\delta t_k := t_{k+1} - t_k$, and d_k a positive random variable independent of W_i :*

$$\tau_i(t_{k+1}) = \tau_i(t_k) + a_i(t_k)\delta t_k + O(\delta t_k^{\frac{3}{2}}), \quad (\text{B-107})$$

$$\tau_i(t_k + d_k) = \tau_i(t_k) + a_i(t_k)d_k + O(\mathbb{E}[d_k^3]^{\frac{1}{2}}), \quad (\text{B-108})$$

$$a_i(t_{k+1}) = a_i(t_k) + O(\delta t_k^{\frac{1}{2}}). \quad (\text{B-109})$$

Proof: Let $a(a_i(t), t) := (-\alpha_i \log a_i(t) + \frac{3\epsilon_i^2}{4}(1 - e^{-2\alpha_i t}))a_i(t)$. From (3), (4) we have

$$\begin{aligned} \tau_i(t_{k+1}) &= \tau_i(t_k) + \int_{t_k}^{t_{k+1}} a_i(t) dt \\ &= \tau_i(t_k) + a_i(t_k)\delta t_k + \int_{t_k}^{t_{k+1}} \int_{t_k}^{t'} a(a_i(s), s) ds dt' + \int_{t_k}^{t_{k+1}} \int_{t_k}^{t'} \epsilon_i a_i(s) dW_i(s) d\mathbf{B} \end{aligned} \quad (\text{B-110})$$

Define $A := \int_{t_k}^{t_{k+1}} \int_{t_k}^{t'} a(a_i(s), s) ds dt'$, $B := \int_{t_k}^{t_{k+1}} \int_{t_k}^{t'} \epsilon_i a_i(s) dW_i(s) dt'$. It is easy to verify that there exists $C_1 > 0$ s.t. $|a(a_i(t), t)| \leq C_1(a_i(t) + a_i^2(t))$. By the fact that $a_i(t)$ is L^p -bounded for all $p \geq 1$ (cf. Lemma 4) and Tonelli's theorem [40], $A = O(\delta t_k^2)$. By Itô's isometry [12] and Fubini's theorem [40],

we get for some constant $C > 0$

$$\begin{aligned}
 \mathbb{E}[B^2] &= \epsilon_i^2 \int_{t_k}^{t_{k+1}} \int_{t_k}^{t_{k+1}} \mathbb{E} \left[\int_{t_k}^{t'} \int_{t_k}^{t''} a_i(s) a_i(r) dW_i(s) dW_i(r) \right] dt' dt'' \\
 &\leq C \int_{t_k}^{t_{k+1}} \int_{t_k}^{t_{k+1}} t' \wedge t'' dt' dt'' \\
 &= O(\delta t_k^3).
 \end{aligned} \tag{B-111}$$

Using the fact that $O(\delta t_k^2) + O(\delta t_k^{\frac{3}{2}}) = O(\delta t_k^{\frac{3}{2}})$ for small values of δt_k establishes (B-107). Applying the same analysis to the conditional expectation given d_k yields $\mathbb{E}[(\tau_i(t_k + d_k) - \tau_i(t_k) - a_i(t_k)d_k)^2 | d_k] = O(\delta t_k^3)$. Taking expectations in both sides establishes (B-108). The proof of (B-109) follows along the same lines using (4), Itô's isometry and the L^p -boundedness of $a_i(t)$. \blacksquare

From (3), we have the following approximation

$$r_{i,j}^{(k)} = \tau_j(t_k) + a_j(t_k)d_{ij}^{(k)} + e_k^{(r)}, \tag{B-112}$$

$$r_{i,j}^{(k+1)} = \tau_j(t_{k+1}) + a_j(t_{k+1})d_{ij}^{(k+1)} + e_{k+1}^{(r)}, \tag{B-113}$$

$$a_j(t_{k+1})d_{ij}^{(k+1)} = a_j(t_k)d_{ij}^{(k+1)} + e_k^{(a)}, \tag{B-114}$$

$$s_i^{(k+1)} - s_i^{(k)} = a_i(t_k)\delta t_k + e_k^{(s)}, \tag{B-115}$$

$$\tau_j(t_{k+1}) - \tau_j(t_k) = a_j(t_k)\delta t_k + e_k^{(j)}. \tag{B-116}$$

From the previous lemma the error terms satisfy $e_k^{(r)} = O(d_{ij}^{(k)\frac{3}{2}})$, $e_k^{(a)} = O(d_{ij}^{(k+1)})O(\delta t_k^{\frac{1}{2}})$, $e_k^{(s)} = O(\delta t_k^{\frac{3}{2}})$, $e_k^{(j)} = O(\delta t_k^{\frac{3}{2}})$. We adopt the following assumptions on the communication delays:

Assumption 1 (Assumption on delays). The delays $\{d_{ij}^{(k)}\}$ are positive random variables upper bounded by D , independent across time instants k , and links (i, j) , and identically distributed across time instants k for a fixed link (i, j) , as well as independent of $\{W_i(t)\}$.

Subtracting (B-112) from (B-113) and using (B-114), (B-116) we get

$$r_{i,j}^{(k+1)} - r_{i,j}^{(k)} = a_j(t_k)\delta t_k + a_j(t_k)(d_{ij}^{(k+1)} - d_{ij}^{(k)}) + O(\delta t_k^{\frac{3}{2}}) + O(d_{ij}^{(k)\frac{3}{2}}) + O(d_{ij}^{(k+1)\frac{3}{2}}) + O(d_{ij}^{(k+1)})O(\delta t_k^{\frac{1}{2}}). \tag{B-117}$$

The goal is to express the Taylor expansion for the fraction $\frac{r_{i,j}^{(k+1)} - r_{i,j}^{(k)}}{s_i^{(k+1)} - s_i^{(k)}}$, i.e., divide (B-117) by (B-115).

$$\frac{1}{s_i^{(k+1)} - s_i^{(k)}} = \frac{1}{(t_{k+1} - t_k)} \frac{1}{\frac{1}{(t_{k+1} - t_k)} \int_{t_k}^{t_{k+1}} a_i(t) dt} \leq \frac{1}{(t_{k+1} - t_k)^2} \int_{t_k}^{t_{k+1}} \frac{1}{a_i(t)} dt, \tag{B-118}$$

where we have used Jensen's inequality. In particular, it follows that for every m , $\delta s_i^{(k)m} := s_i^{(k+1)} - s_i^{(k)} = \Theta(\delta t_k^m)$; the sender can directly control $\delta s_i^{(k)}$. By the Taylor expansion of $g(x) = \frac{1}{c+x}$, $c > 0$ around $x = 0$ and (B-115):

$$\frac{1}{s_i^{(k+1)} - s_i^{(k)}} = \frac{1}{a_i(t_k)\delta t_k} + \frac{O(\delta t_k^{\frac{3}{2}})}{\Theta(\delta s_i^{(k)2})} = \frac{1}{\delta t_k} \frac{1}{a_i(t_k)} + O(\delta t_k^{-\frac{1}{2}}), \quad (\text{B-119})$$

whence

$$\frac{r_{i,j}^{(k+1)} - r_{i,j}^{(k)}}{s_i^{(k+1)} - s_i^{(k)}} = \frac{a_j(t_k)}{a_i(t_k)} \left(1 + \frac{d_{ij}^{(k+1)} - d_{ij}^{(k)}}{\delta t_k}\right) + e_k, \quad (\text{B-120})$$

$$e_k = O(\delta t_k^{\frac{1}{2}}) + O(d_{ij}^{(k+1)})O(\delta t_k^{-\frac{1}{2}}) + [O(d_{ij}^{(k)\frac{3}{2}}) + O(d_{ij}^{(k+1)\frac{3}{2}})]O(\delta t_k^{-1}), \quad (\text{B-121})$$

or, equivalently, (by the first-order Taylor expansion of $\log(c+x)$, $c > 0$)

$$\log \left| \frac{r_{i,j}^{(k+1)} - r_{i,j}^{(k)}}{s_i^{(k+1)} - s_i^{(k)}} \right| = -\frac{1}{4} \left(\frac{\epsilon_j^2}{\alpha} - \frac{\epsilon_i^2}{\alpha} \right) (1 - e^{-2\alpha t_k}) + X_{ij}(t_k) + \log \left| 1 + \frac{d_{ij}^{(k+1)} - d_{ij}^{(k)}}{t_{k+1} - t_k} \right| + e'_k, \quad (\text{B-122})$$

$$e'_k = O(\delta t_k^{\frac{1}{2}}) + O(d_{ij}^{(k+1)})O(\delta t_k^{-\frac{1}{2}}) + [O(d_{ij}^{(k)\frac{3}{2}}) + O(d_{ij}^{(k+1)\frac{3}{2}})]O(\delta t_k^{-1}), \quad (\text{B-123})$$

The quantity $y_{ij}(t_k) := \log \left| \frac{r_{i,j}^{(k+1)} - r_{i,j}^{(k)}}{s_i^{(k+1)} - s_i^{(k)}} \right|$ can be obtained from measurements. Note that because of delay variation, it might be that $r_{i,j}^{(k+1)} < r_{i,j}^{(k)}$, even though $s_i^{(k+1)} > s_i^{(k)}$, so the use of absolute value in the definition of $y_{ij}(t_k)$ is indispensable; this corresponds to out-of order delivery of packets in wireless. The quantity $v_{ij}(t_k) := \log \left| 1 + \frac{d_{ij}^{(k+1)} - d_{ij}^{(k)}}{t_{k+1} - t_k} \right| + e'_k$ is random, and depends on the rate of delay variations and the skew variations during the send times of the two consecutive packets. Hence we get

$$y_{ij}(t_k) := X_{ij}(t_k) + v_{ij}(t_k). \quad (\text{B-124})$$

It is well known [12], that linear filtering is the only computationally tractable estimation scheme for the state equation (1). Hence, we need to model $v_{ij}(t_k)$ as white Gaussian noise, i.e., $v_{ij}(t_k) \sim \mathcal{N}(0, \sigma_{ij}^2(t_k))$. Note that the random variables $\{e'_k\}$ are not independent across time, because $a_{ij}(t)$, $X_{ij}(t)$ are not independent increment processes. However, if we further make the assumption that link delays can be made small (for a practical scheme to reduce delays via proper time-stamping see [19]), in particular assuming that $d_{ij}^{(k)m} = O(\delta t_k^m)$, $m = 1, \frac{3}{2}$ implies that $e'_k = O(\delta t_k^{\frac{1}{2}})$. Therefore we ignore the correlation between e'_k for different values of k , as it can be controlled by δt_k . By the assumption of small delays, it is reasonable to assume that the variance sequence is uniformly upper bounded and the variance $\sigma_{ij}^2(t_k)$ is an increasing function of δt_k , of the known quantity $\delta s_i^{(k)}$. ■